Journal of Industrial and Engineering Chemistry 98 (2021) 17–41

Contents lists available at ScienceDirect

Journal of Industrial and Engineering Chemistry

journal homepage: www.elsevier.com/locate/jiec

Review

Zeolitic imidazolate framework membranes for gas separations: Current state-of-the-art, challenges, and opportunities

Mohamad Rezi Abdul Hamid[a,*], Thomas Choong Shean Yaw[a], Mohd Zahirasri Mohd Tohir[a], Wan Azlina Wan Abdul Karim Ghani[a], Putu Doddy Sutrisna[b], Hae-Kwon Jeong[c,*]

[a] Department of Chemical and Environmental Engineering, Faculty of Engineering, Universiti Putra Malaysia, Serdang, Selangor 43400, Malaysia
[b] Department of Chemical Engineering, Faculty of Engineering, University of Surabaya (UBAYA), Surabaya, Indonesia
[c] Artie McFerrin Department of Chemical Engineering and Department of Materials Science and Engineering, Texas A&M University, College Station, TX 77843-3122, United States

ARTICLE INFO

Article history:
Received 6 March 2021
Received in revised form 27 March 2021
Accepted 30 March 2021
Available online 7 April 2021

Keywords:
Metal organic frameworks
Zeolitic imidazolate frameworks
Membranes
Gas separations
Hollow fibers

ABSTRACT

Advanced porous materials with uniform molecular scale apertures are highly desirable for energy related separations. Among them, zeolitic imidazolate frameworks (ZIFs) have received significant interest as separation membranes owing to their narrow apertures that can target small gases. ZIFs exhibit excellent gas transport properties, such as unprecedentedly high C_3H_6 permeability and remarkable C_3H_6/C_3H_8 selectivity, inaccessible by other porous inorganic materials and polymers. Deposition of ultrathin ZIFs on porous substrates to form gas-selective barriers has been a major focus in this area. There has been a significant development in the synthesis of ultrathin ZIF membranes for gas separations. In this review, we present a summary of current state-of-the-art in ZIF membrane processing and highlight unique microstructural features of the prepared membranes. Following this, we discuss level of separation performances of these advanced membranes focusing on three emerging/unsolved applications. Finally, we provide our perspectives on future research directions in the area.

Contents

* Corresponding authors.
E-mail addresses: m_rezi@upm.edu.my (M.R. Abdul Hamid), hjeong7@tamu.edu (H.-K. Jeong).

https://doi.org/10.1016/j.jiec.2021.03.047
1226-086X/

Introduction

Separation and purification of chemical mixtures are important steps in modern chemical industries, accounting for roughly 10–15% of the global energy consumption [1,2]. Development of more energy efficient chemical separation processes could save billions of dollars of energy cost and reduce greenhouse gas emission [1]. Membrane-based technology is a promising energy efficient alternative over the conventional thermally-driven processes to purify industrially important gases. Gas separations by membranes require less energy and investment cost compared to other competing technologies including distillation, adsorption, and absorption [3,4]. Scholl and Lively [1] estimate that membrane-based separations use 90% less energy compared to the distillation. Among other advantages of membranes are low energy consumption, operational flexibility (meaning that the membrane can work as a standalone unit or retrofitted into existing process unit), small carbon footprint, and linear scale up (applicable for small and medium scale processes) [5–9].

Membrane technology is a fairly mature technology but is still expanding. Membrane technology has a projected market value of $2.6 billion in 2022, ~86% higher than the market value back in 2018 [6,10]. The majority of commercial gas separation membranes are polymer based, in which 90% of them are intended for the separation of non-condensable gases such as hydrogen (H_2) purification, nitrogen (N_2) production from air, and natural gas treatment [4,10,11]. Polymers are a versatile class of material with diverse functionalities and excellent processabilities [12]. They are inexpensive and can be formed as flat sheets or hollow fibers with effective skin layer thicknesses of less than 100 nm using phase separation techniques and their variance [11]. Polymers however suffer from the permeability-selectivity trade-off [13]. In other words, highly permeable polymers will possess low selectivity and vice versa. The trade-off relationship represents a challenge among membrane scientists to develop polymer membranes with high permeabilities and selectivities. While there have been some improvements made over the recent years, only a marginal shift in the upper bound was observed [14]. Polymers also suffer from swelling and plasticization issues which typically occur at elevated pressures compromising membrane separation performances [15–17]. It is also worthy of mentioning that 90% of the commercial polymer membranes are made from less than 10 polymer materials (e.g., cellulose acetate, polyimide, polysulfone, polycarbonate, and silicone rubber) which most have been used for the last four decades [18].

Other than the big four commercial membrane applications (i.e., H_2 purification, N_2 production from air, natural gas treatment, and vapor recovery), a much larger potential market for membranes are in the separations of condensable gases such as methane (CH_4) recovery from heavier hydrocarbons and olefin/paraffin separations (e.g., ethylene/ethane, propylene/propane, and *n*-butane/i-butane) [4]. For instance, separation of olefin from their respective paraffin is one of the largest gas-phase separations in chemical industries typically achieved through low temperature distillation. Ethylene (C_2H_4) and propylene (C_3H_6) are the two largest chemical commodities in chemical/petrochemical industries with a combined annual production of 2.9×10^8 metric tons [19]. C_2H_4 and C_3H_6 are important chemical feedstocks for the production of a wide variety of intermediates and polymers. For production of polymers (e.g., polyethylene and polypropylene), C_2H_4 and C_3H_6 purity of 99.9 mol% and 99.5 mol%, respectively, are required [20,21]. Olefin/paraffin separations using polymer membranes are challenging due to similar physical and chemical properties of the penetrants. Moreover, poorly defined free volume

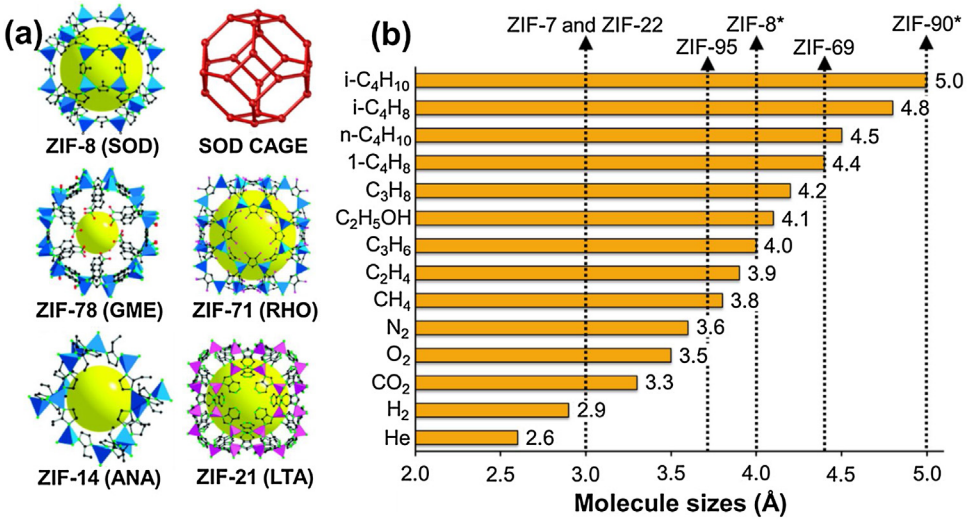

Fig. 1. (a) Example of crystal structures of ZIFs. Adapted with permission from Ref. [38] Copyright 2009 American Chemical Society (b) Comparison of the pore apertures of ZIFs (XRD-derived or effective apertures) with molecular sizes of penetrants. In this figure, hybrid molecular dimensions (kinetic diameter and Van der Waals) are used to represent molecular sizes of penetrants. Penetrant sizes are taken from Ref. [39] and * symbol represents effective aperture of ZIFs.

of polymers result in low diffusional selectivity [5]. To address the shortcoming of polymers, researchers have begun investigating other types of membrane materials such as zeolites [22], carbon molecular sieves [23], graphene [24], and metals [25]. Generally speaking, inorganic microporous membranes possess better gas transport properties than those of polymer membranes in addition to having superior chemical and thermal stabilities.

Metal organic frameworks (MOFs) are hybrid organic-inorganic porous materials designed by bridging inorganic metals or metal-containing clusters and organic linkers through coordination bonding [26–28]. MOFs are well known for having uniform molecular scale apertures, large internal surface areas (1,000–10,000 $m^2 g^{-1}$), high porosities (up to 90% pore volume), and tailorable pore sizes and internal surfaces [29,30]. Unique properties of MOFs have drawn considerable attention for a wide variety of technological applications including gas storage [31], chemical separations [32], catalysis [33], gas sensing [34], and drug delivery [35]. Zeolitic imidazolate frameworks (ZIFs), a subset of MOFs, are constructed by bridging divalent metal ions (e.g., Zn^{2+}, Co^{2+}, Cd^{2+}, etc.) with imidazole-based linkers to form three-dimensional networks with zeolite topologies (e.g., SOD, MER, LTA, RHO, etc.) as depicted in Fig. 1(a) [36,37]. ZIFs are thermally stable up to 550 °C and chemically inert in various solvents including alkaline water and organic solvents [37].

Most ZIFs have pore sizes of less than 5.0 Å which are in the size range of small molecules. Among the ZIF structures that are available, SOD-type ZIFs such as ZIF-7 (0.30 Å) [37], ZIF-8 (0.34 Å) [37], ZIF-9 (<0.34 Å) [37], ZIF-67 (0.33 Å) [40], and ZIF-90 (0.35 Å) [41] is the most relevant ZIF topology for small gas sieving. The SOD cage of ZIFs is shown in Fig. 1(a). Narrow six-membered rings of the cage provide high gas diffusion selectivity while large open cavities guarantee high gas diffusion through the frameworks. Thermally activated flip-flopping motions of imidazole ligands enlarges the pore apertures of ZIFs beyond its XRD-derived values. Effective aperture of ZIF-8 was found to be much larger (4.0–4.2 Å) than its XRD-derived aperture of 3.4 Å, attributable to the rotation of 2-methylimidazole linkers [39]. Meanwhile, ZIF-90 has effective aperture of ~5.0 Å, much larger than its nominal aperture of 3.5 Å [42]. Being crystalline materials, ZIF suffer from having discreet and limited available apertures as shown in Fig. 1(b). In other words, ZIFs usability are limited to a particular gas mixture and cannot be used to efficiently separate other gases.

Researchers typically go around this fundamental limitation of ZIFs by adopting a hybrid approach. Incorporation of secondary metals or linkers into parent ZIF structures either through de novo approach or post-synthetic modification (PSM) modifies the transport properties of ZIFs to target other gas mixtures which previously inaccessible when using pure ZIFs [42–48]. Prior research on ZIFs has mostly focused on the discovery, characterization, and utilization of the materials in their powder/bulk form. However, over the recent years there have been particularly significant developments in ZIF membrane synthesis for separation applications with various innovative strategies proposed [49–54]. As illustrated in Fig. 2, the number of publications on ZIF-based membranes for gas separations have steadily risen. The list of ZIFs being investigated as separation membranes includes ZIF-7, ZIF-8, ZIF-9, ZIF-22, ZIF-67, ZIF-78, ZIF-90, ZIF-93, ZIF-95, and ZIF-100 among others, with ZIF-8 being the most widely investigated ZIFs.

There are two approaches adopted by researchers to utilize ZIFs for separation applications. First strategy is to embed preformed ZIF nanocrystals into a continuous polymer matrix to form what is known as mixed-matrix membranes (MMMs). MMMs are composite materials consisting of zero-, one- or two-dimensional inorganic nanofillers (typically more selective), dispersed homogenously in a continuous polymer phase [5]. Unlike the purely inorganic zeolites, organic linkers of ZIFs provide better interaction

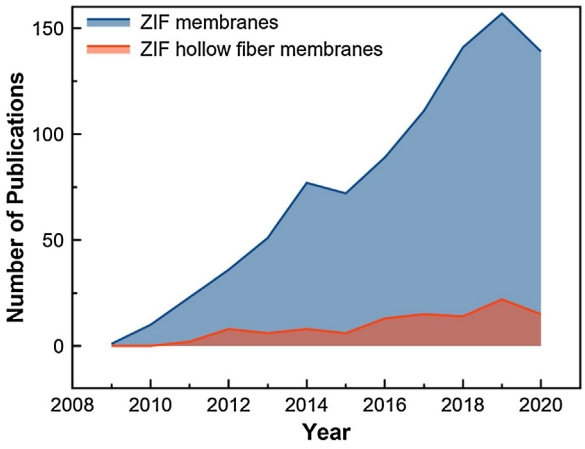

Fig. 2. Number of publications per year with phrase "zeolitic imidazolate framework (ZIF) membranes" and "zeolitic imidazolate framework (ZIF) hollow fiber membranes" since 2009. Data obtained from Web of Science (December 2020).

with polymer matrix, resulting in a more intimate interface. MMMs combine desirable properties of both polymer and inorganic phases [55]. Open frameworks and size-selective nature of ZIF fillers allow for improvement in composite membrane permeability and selectivity while maintaining low cost and processing convenience of polymer. For ZIF-based MMMs, there have been several interesting discoveries made. For instance, Park et al. [56] managed to in-situ transform sub-1 μm thick (750 nm) premade 6FDA-DAM (4,4′-(hexafluoroisopropylidene) diphthalic anhydride-2,4,6-trimethyl-1,3-diaminobenzene) polyimide coating on commercial polyethersulfone hollow fibers and α-alumina discs into ZIF-8/6FDA-DAM MMMs using what they refer to as the polymer-modification-metal-organic-framework-formation (PMMOF) technique. The PMMOFed MMMs showed impressively high propylene/propane (C_3H_6/C_3H_8) separation factor as high as 38.0 ± 7.1 satisfying the commercial requirement despite using lower volume fraction of ZIF-8 (32.9 vol%). Though interesting, the subject of MOF/ZIF-based MMMs for gas separations is better left for another discussion. Moreover, there are many excellent reviews already available to keep the reader updated on the subject matter [57–61].

Second strategy to utilize ZIFs for separation applications is to grow a continuous and defect-free polycrystalline ZIF layer. Polycrystalline ZIF membranes are usually considered as inorganic membranes because their structures, synthesis, and gas transport properties are similar to those of inorganic zeolites [62]. Since free standing ZIFs possess low mechanical strength, the molecular sieve layers are usually grown on porous supports (e.g., ceramic, polymer, and metal) to provide mechanical strength [63]. Unlike ZIF-based MMMs which show moderate improvement in both permeability and selectivity, separation performances of pure ZIF membranes are significantly higher. However, a major challenge is to fabricate large area and defect-free ZIF polycrystalline layers on porous substrates in cost-effective manner. There have been significant developments in this area in the past years. Despite the rising interest, the number of published works on ZIF membranes on industrially relevant substrates (i.e., hollow fiber, capillary, and tube) is still low. This is no surprise considering the difficulties in preparing high quality ZIF membranes on these substrates, especially on the lumen side of the fibers, compared to planar substrates.

Herein, we present a systematic review of current state-of-the-art in polycrystalline ZIF membranes synthesis, their applications in gas separations, and the reported separation performances. A selection of research works reported within the last five years has

become the main focus of this review. The applications of ZIF membranes included in the discussion are limited to three unsolved applications in gas separation membranes (e.g., H_2 purification, CO_2 removal, and olefin/paraffin separations). There are several noteworthy reviews on ZIF membranes for gas separations already available in literature [49–54]. To set our work apart, we decided to put more emphasis on the preparation of ZIF membranes on high packing substrates, which is a less popular subject in the field. We then provide commentaries on several technical challenges in ZIF membrane synthesis and conclude by highlighting future research direction on the development of pure/hybrid ZIF membranes targeting other gas mixtures. We hope that the current contribution could provide meaningful insights and ideas for the design of high performance gas separation membranes. We also hope to inspire membrane scientists to come out with innovative solutions to fabricate high performance ZIF membranes in a cost-effective manner.

Zeolitic imidazolate framework (ZIF) membranes

A scalable ZIF membrane concept

Fig. 3 summarizes important criteria for what we believe to be a scalable and economically attractive ZIF membrane concept. Selecting membrane materials with proper gas permeability and selectivity is the first step towards industrial scale deployment of gas separation membranes. Economics of the membrane system rely heavily on membrane transport properties. Highly selective and highly permeable membranes guarantee high purity product with high recovery rate using less membrane area [12]. ZIFs being crystalline materials offer good selectivity and permeability for a specific gas mixture. For instance, ZIF-8 offers high intrinsic C_3H_6 permeability of 390 Barrer and permselectivity of 130; an ideal candidate for C_3H_6/C_3H_8 separations ($1\ \text{Barrer} = 3.348 \times 10^{-16}$ mol m m^{-2} s^{-1} Pa^{-1}) [39]. While this aspect of gas separation membranes is largely resolved through a proper ZIF selection, one should note that no matter how permeable the selected ZIF is, it must be fabricated into a thin (sub-1 μm thick) and defect-free layer to achieve high gas fluxes [18]. In commercial gas separation plants, the required membrane area is in the order of several hundred thousands of square meter (1,000–500,000 m^2) [18]. Increasing membrane productivity is critically important for ZIF membranes as the membranes are likely to have higher fabrication cost compared to polymer membranes. Highly productive membranes require smaller membrane area to perform the required separation. Capital investment for membrane installations can therefore be reduced to a point where it can be as economically attractive as the traditional polymer membranes.

Membrane productivity, which is the core idea of this review is defined as a molar flow rate of feed gases that a membrane can process per unit time (mol s^{-1}). The productivity of a membrane can be expressed using the following equation:

$$Q_i = -P_i A \frac{\Delta p_i}{l} \quad (1)$$

where P_i, A, l and Δp_i are permeability of gas i (mol m m^{-2} s^{-1} Pa^{-1}), membrane area (m^2), membrane thickness (m), and partial pressure difference of gas i between feed and permeate sides (Pa), respectively. Q_i that is the amount of gases that a membrane can process per unit time (mol s^{-1}) depends on membrane thickness and surface area. Theoretically, one can achieve a ten-fold membrane productivity increase by reducing membrane thickness from 1 μm to 0.1 μm. Productivity increase can also be achieved by increasing membrane surface area. In other words, synthesizing the membrane on high surface-to-volume modules such as hollow fibers. Hollow fibers can provide high packing density up to 13,000 m^2 m^{-3}. Fabricating ZIF membrane on high packing modules and/or reducing membrane thickness, ideally to sub-0.1 μm range are among the areas currently addressed by membrane researchers. However, it should be reminded that neither of these strategies is straightforward with only a few lab scale successes reported.

Scalable ZIF membranes must have excellent reproducibility, robust synthesis, and ability to be fabricated into modules in a cost-effective manner. In addition, the membranes must have excellent chemical and thermal stabilities especially for those that will be used under chemically aggressive and high temperature conditions. The cost of inorganic membranes are still expensive. According to Lin et al. [62], the cost of inorganic membranes grown on ceramic microfiltration membranes is anywhere between $1,000–5,000 per m^2. For comparison, the cost of polymer membranes is $5 and $10 per m^2 for hollow fiber and flat geometry, respectively [64]. In some studies, polymers have been used to replace inorganic supports in the synthesis of ZIF membranes aiming to reduce membrane cost. However, the supports generally do not have good thermal and chemical stabilities. Inorganic supports including alumina, titania, zirconia, and metal are fairly

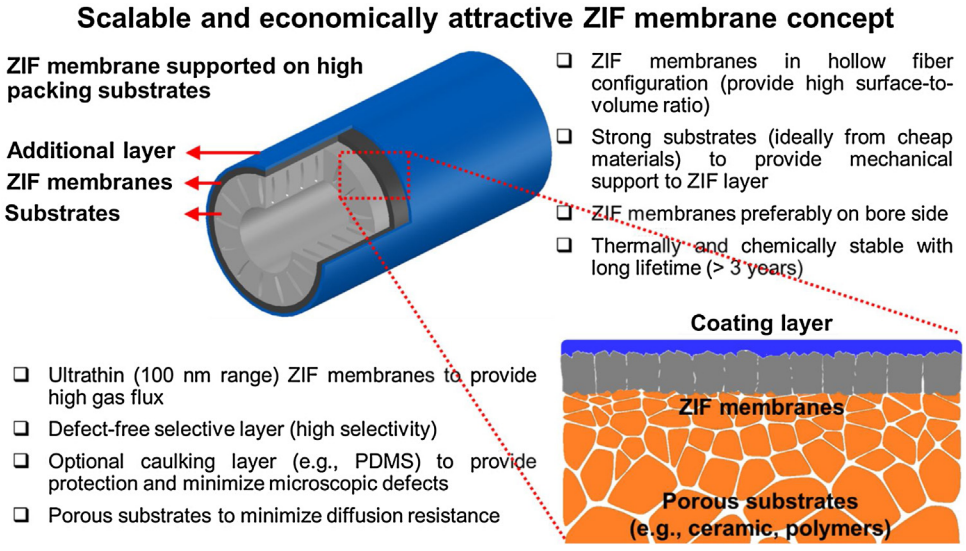

Fig. 3. Schematic illustration and criteria for a scalable and commercially attractive ZIF membrane concept.

expensive, contributing to roughly 80% of the overall membrane cost [65]. Nevertheless, the long term cost saving from having chemically and thermally resilient supports might favor the selection of inorganic supports over organic supports [64]. Finally, industrially relevant ZIF membranes must have long membrane lifetime of at least three to five years [18]. At present, difficulty in preparing defect-free ultrathin large area membranes, low module packing density, high manufacturing cost, and modest reproducibility are among the barriers that prevented the commercial scale deployment of ZIF membranes [62].

General synthesis strategy (in-situ vs. secondary growth)

Fabrication protocols of ZIF thin films and membranes generally follows that of zeolite membranes as both are porous crystalline materials [9]. ZIF membranes can be prepared via in-situ method or secondary (seeded) growth method. In-situ synthesis is a more popular choice among researchers to prepare polycrystalline membranes as the preparation steps is less complicated [50]. Meanwhile, secondary growth can provide better control over membrane microstructures (e.g., crystal orientation, crystal sizes, thickness, grain boundary structures, etc.) which consequently affect the membrane transport properties [66].

As illustrated in Fig. 4(a), in-situ synthesis is a one-step solvothermal or hydrothermal membrane formation on porous substrates without pre-attached seed crystals. Unlike the secondary growth strategy, in-situ synthesis does not require complicated preparations, making it attractive for scale up. Traditionally, in-situ membrane synthesis is achieved by directly immersing bare, surface modified, or metal saturated supports in a synthesis solution for a predetermined period. To date, various synthesis protocols have been devised for the preparation of polycrystalline ZIF membranes including direct solvothermal growth [67], layer-by-layer deposition [68,69], counter-diffusion [70,71], microwave synthesis [43,72], electrospray deposition [73,74], interfacial growth [75,76], and solvent/solvent-free zinc oxide transformation [77–79] along with other techniques. In-situ synthesis has been applied to prepare a wide variety of ZIF structures including ZIF-7 [74,80], ZIF-8 [67,81], ZIF-9 [82], ZIF-22 [83], ZIF-67 [84], ZIF-78 [85], ZIF-90 [86,87], ZIF-93 [88], ZIF-95 [89], ZIF-100 [90], mixed-metal ZIFs (e.g., Co–Zn–ZIF-8 [91,92]), and mixed-ligand ZIFs (e.g., 2-ethylimidazole-ZIF-8 [93], benzimidazole-ZIF-8 (ZIF-7-8) [94], and 2-imidazolecarboxaldehyde-ZIF-8 (ZIF-8-90) [95]).

Inorganic ceramics, metals, and polymers are among the most commonly used substrates for in-situ ZIF membrane synthesis. They, however, are relatively inert providing low heterogeneous nucleation density [96–99]. Physical or chemical functionalization are often introduced to promote and direct heterogeneous nucleation and growth of ZIFs on preferred surfaces. Decorating support surfaces with reactive groups such as amino [82,100], hydroxyl [96,101,102], and imidazoline [69,103] groups improves heterogeneous nucleation of ZIFs owing to their ability to form complexes with metal ions. These surface groups are expected to promote better adhesion between ZIF layers and supports through covalent (e.g., Zn–N) or noncovalent bonds which result in mechanically strong membranes [83,87,104]. 3-aminopropyltriethoxysilane (APTES) surface modifications have been employed to fabricate tightly packed ZIF polycrystalline layers [82,100]. Following a similar concept, Jiang et al. [101] and Ruan et al. [102] functionalized surface of anodized aluminum oxide (AAO) and α-Al_2O_3 discs, respectively, with polydopamine bio-adhesives to fabricate highly permselective ZIF-8 membranes.

In the traditional in-situ synthesis, crystal nucleation and growth occur simultaneously, providing small window for independent optimizations. It is therefore quite challenging to control microstructures of the ZIF membranes prepared using this approach. Take solution-based-counter-diffusion method as an example. Ideally, 'metal-ligand reaction zone' should occur at the vicinity of the substrates [67]. Slow precursor diffusion rates relative to reaction rates lead to a formation of thick membranes inside the supports, which reduce the membrane fluxes. On the other hand, high precursor diffusion rates relative to reaction rates lead to homogenous nucleation resulting in discontinuous membranes with macroscopic voids [105]. Nucleation densities of ZIF on support surfaces determine minimum thickness of the resulting membranes (i.e., low nucleation densities on supports produce thick membranes and vice versa).

From our review, we noticed that researchers have begun to move away from the traditional solution-based in-situ synthesis. A few of them have begun considering solvent-less routes to prepare ZIF membranes. These new methods not only simpler and faster, but also able to produce ZIF membranes with thickness of less than 100 nm. We will review these innovative strategies in detail in the following section.

Secondary growth is an approach widely used in the synthesis of inorganic zeolite membranes which later applied to ZIF membrane synthesis [108–110]. As opposed to the in-situ method, secondary growth is a two-steps process which involves the deposition of high quality seed crystals on substrates followed by hydrothermal or solvothermal growth where the seed crystals

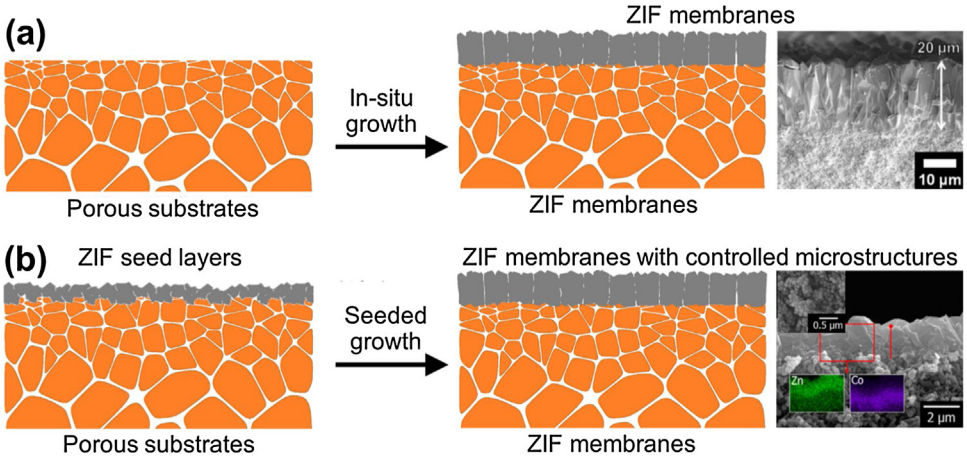

Fig. 4. Comparison between (a) in-situ growth and (b) secondary seeded growth for ZIF membrane synthesis. Inset electron image shows densely packed ZIF-8 seed layers deposited on α-Al_2O_3 substrates using microwave heating. Modified with permission from Ref. [106] Copyright 2010 and Ref. [107] Copyright 2015 American Chemical Society.

grow and later form coherent films. In general, high quality seed layers consist of densely-packed seeds with uniform surface coverage and strong anchorage to support surfaces (see Fig. 4(b), inset). The seed layers can be obtained through manual rubbing [111], dip/slip coating [44,92,112], reactive seeding [85,113], microwave seeding [91,107,114], and thermal seeding [115]. A densely packed ZIF seed layer deposited on substrate enables the formation of a thin membrane. In most cases, the majority of ZIF membranes prepared using the secondary growth method are relatively thin with thicknesses of 2–3 μm at most [91,107,116–120]. Despite more complicated, nucleation and growth steps in secondary growth are decoupled, allowing each step to be optimized independently. Therefore, one has the freedoms to manipulate important nucleation and growth parameters to obtain membranes with desired microstructures. For instance, Bux et al. [121] managed to grow ~12 μm thick ZIF-8 membranes with (110) plane preferred orientation by varying the secondary growth time. Liu et al. [122] manipulated secondary growth synthesis recipe to favor crystal growth along *c*-direction to form highly *c*-oriented ZIF-69 membranes on porous α-Al_2O_3 discs.

State-of-the-art in ZIF membrane synthesis for gas separations

Reducing ZIF membranes thickness. What is the limit?

One of the pressing issues in zeolite membranes, MOF and ZIF membranes included, is high cost stemming from the use of expensive inorganic supports [3,123]. Cheaper substrates such as polymers can reduce membrane manufacturing cost to some extent, but then again, thermal and chemical stability of the polymers give rise to new problems. Experts believe that a true solution behind this matter is productivity increase to a point where the capital cost of setting up inorganic membranes is economically as attractive to polymer membranes [124]. For practical purposes, increasing membrane flux (by decreasing membrane thickness) is likely the only way forward to justify the relatively high cost of inorganic membranes [95]. One of the major goals in inorganic membrane community is to synthesize highly selective ZIF membranes with thickness in the sub-100 nm range. Tsapatsis [124] estimated that for certain applications, membrane thickness need to be even further decreased to ~50 nm. While this goal may seem out of our reach about a decade ago, several recently published works have demonstrated that synthesizing sub-100 nm thick ZIF membranes is no longer unattainable.

Fig. 5 shows important milestones in the development of ultrathin ZIF membranes made in the past decade. To the best of our recollection, the first ever ZIF membranes for gas separation is a 38 μm thick ZIF-8 membrane prepared via microwave synthesis in 2009 [72]. The application of secondary growth method in the synthesis of ZIF membranes drastically reduce membrane thickness to 1–3 μm [107,114,120]. Developments of sub-1 μm thick ZIF membranes appear in the latter half of the decades which consequently shifting membrane productivity toward higher values. Shamsaei et al. [131] prepared ultrathin ZIF-8 membranes with thickness of 200 nm on bromomethylated poly(2,6-dimethyl-1,4-phenylene oxide) substrates using a chemical vapor modification method. Kwon et al. [126] took advantage of the Ostwald-ripening like process of the ZIF-8 nanocrystals in a ligand vapor environment to fabricate 300–400 nm thick membranes for C_3H_6/C_3H_8 separations. Recently published work by Qiao et al. [129] reported ultrathin ZIF-8 membranes with thickness of only 45 nm, exhibiting unprecedentedly high C_3H_6 permeance of 3,000 GPU (1 GPU = 3.348×10^{-10} mol m^{-2} s^{-1} Pa^{-1}). For comparison, C_3H_6 permeance of 1–2 μm thick ZIF-8 membranes are in the range of 30–60 GPU only. The record for thinnest ZIF membranes for gas separations was a ~17 nm thick ZIF-8 membrane synthesized by Li et al. [130]. Based on the current trend, it is not unrealistic to expect ZIF membranes in the coming years to have thickness of only several unit cells.

From our review, we observed a departure from conventional solvent-based membrane synthesis to solvent-free routes which currently gaining popularity. Room temperature, open environment, and flow synthesis have begun to slowly displace the high temperature autoclave-based synthesis. There are also a few scientific works attempting to synthesize ZIF membranes on hollow fibers and tubes, especially on the bore space of the fibers [76,86,116,117,132]. In addition to thickness reduction, we also observed significant reduction in ZIF synthesis time. ZIF membrane synthesis which a decade ago takes a few hours to complete can now be synthesized in just under 10 min [133]. Hillman et al. [43] reported 1 μm thick hybrid ZIF-7-8 membranes prepared in just under 90 s, the fastest ZIF membrane preparation up to date. The above-mentioned advances are an interesting development in the area.

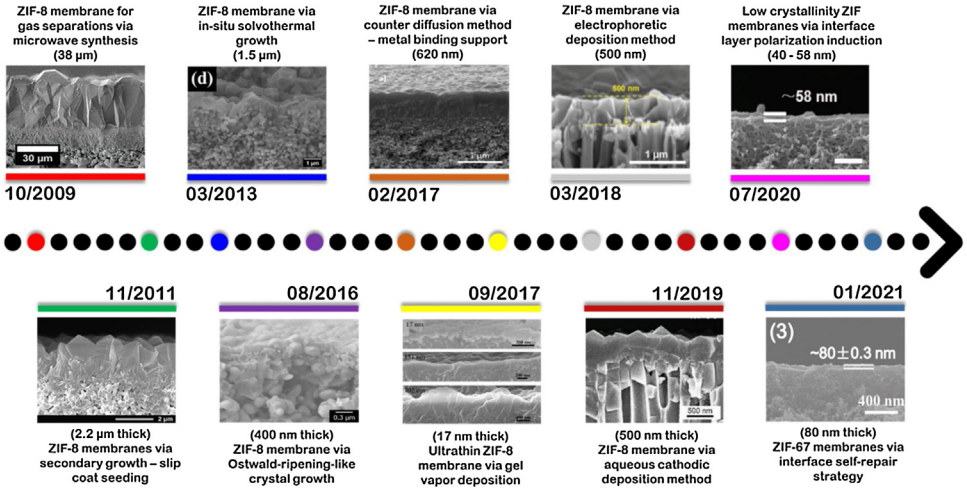

Fig. 5. Important milestones in the development of ultrathin ZIF membranes made since 2009. Note that the major advances in the synthesis of sub-500 nm thick ZIF membranes were mostly reported in latter half of the decades (last five years). Reprinted with permission from Refs. [72] and [67] Copyright 2009 and Copyright 2013 American Chemical Society; reprinted with permission from Refs. [119] and [125] Copyright 2011 and Copyright 2021 Elsevier B.V; reprinted with permission from Ref. [126] Copyright 2016 Royal Society of Chemistry; reproduced with permission from Refs. [71,127,128,129], Copyright 2017, Copyright 2018, Copyright 2019, and Copyright 2020 Wiley VCH; reproduced with permission from Ref. [130] Copyright 2017 Springer Nature.

In this section, we review current state-of-the-art in ultrathin (sub-1 μm thick) ZIF membrane synthesis for gas separations. Emphasis will be put to those grown on high surface-to-volume substrates (e.g., hollow fibers). The state-of-the-art in ZIF membrane synthesis is divided into four categories: (i) interfacial synthesis, (ii) continuous flow processing, (iii) solvent-free vapor phase synthesis, and (iv) current-driven synthesis. We should emphasize that the ZIF membranes prepared using the above-mentioned methods not only innovative but also show state-of-the-art separation performances surpassing majority of reported results prior.

Interfacial synthesis

Interfacial synthesis takes advantage of the immiscibility of solvents to confine ZIF crystallization selectively at the interface between the two solvents. A key requirement behind this method is a selection of solvents with appropriate solubility towards organic and inorganic precursors. Upon contact, the precursors inter-diffuse towards the respective immiscible phases and subsequently crystallize at the liquid–liquid interface. Continuous ZIF layer itself later becomes a diffusion barrier between the solvents thus limit the liquid–liquid interface only at large inter-crystalline gaps [76]. To date, a number of ZIF membranes (e.g., ZIF-8 [75,76,132,134,135] and ZIF-90 [86]) have been prepared using this strategy. Different solvent interfacial systems have been investigated and in most cases the membranes were prepared under relatively mild synthesis conditions (50–70 °C).

Interfacial microfluidic membrane processing (IMMP) developed by Brown et al. [76] utilized 1-octanol/water interfacial system to prepare ZIF-8 membranes on Torlon® polyamide-imide hollow fibers for H_2 purification and C_3H_6/C_3H_8 separation. Zn (dissolved in 1-octanol) and 2-methylimidazole (dissolved in water) solutions were passed through the bore and shell side of the hollow fibers housed inside a custom-made reactor. Two synthesis variables were found important to prepare defect-free ZIF-8 membranes: flow configurations (static, continuous, or combination of both) and initial synthesis conditions. For example, static flow of Zn/1-octanol solution did not produce continuous ZIF-8 films due to insufficient Zn ions in bore space of the hollow fibers [76]. The ZIF-8 membranes supported on hollow fibers, after optimization steps, were well-adhered to substrates and had a uniform thickness of 8.8 μm. Control over membrane microstructures and optimization of IMMP synthesis conditions in their follow up works resulted in ZIF-8 membranes with similar thickness but with much improved C_3H_6/C_3H_8 separation performances [132,135]. Recently, IMMP was used to fabricate all nanoporous MFI/ZIF-8 MMMs (8.0 μm thick) on the bore space of poly (amide-imide) hollow fibers for C_3H_6/C_3H_8 separations (see Fig. 6(a)) [136]. Crystalline MFI zeolites with an average particle size of 141 nm were dispersed in crystalline ZIF-8 matrix to prepare all nanoporous crystalline MMMs. Energy dispersive X-ray elemental mapping was used to determine dispersion of the zeolite particles. Incorporation of medium pore MFI zeolites (channel pore size of 5.5 Å) in crystalline ZIF-8 matrix boosted the membrane permeabilities without sacrificing the intrinsic selectivity of ZIF-8 [137]. The silicalite-1 particles were first treated with 1,3-diaminopropane to functionalize silanol defects of the crystals [138]. The particles were then dispersed in Zn/1-octanol solution and later passed through bore of the hollow fiber at a flow rate of 10 μL h^{-1} (aqueous 2-methylimidazole on shell side) to form the hybrid MFI/ZIF-8 membranes.

In a different study, Biswal et al. [75] took advantage of the liquid–liquid interface between isobutyl-alcohol and water to prepare ZIF-8 and Cu-BTC MOF (BTC, 1,3,5-benzenetricarboxylic acid) membranes on porous PBI-BuI hollow fibers for helium separation. Simple manipulation of the location of metal and linker precursors inside the synthesis module enabled formation of membranes on either side of the hollow fibers. The as-synthesized ZIF-8 membranes were relatively thick: ~10 μm thick for ZIF-8 membrane grown on the bore side and ~20 μm thick for ZIF-8 membrane grown on the shell side. It is noted that isobutyl-alcohol with lower boiling temperature than that of 1-octanol (108 vs. 195 °C) allows the solvent to be removed from ZIF-8 cavities using milder activation temperature.

For gas separation applications, ZIF-8 is not the only material of interest here. There are a range of ZIFs for gas separation applications. However, solubility problems between ZIF precursors and solvents may limit not only the types of ZIF membranes to be prepared but also limit types of materials to be used as substrates [140]. For instance, ZIF-7 synthesis requires polar aprotic solvents (e.g., *N*-methyl-pyrrolidinone and dimetylformamide). Under this

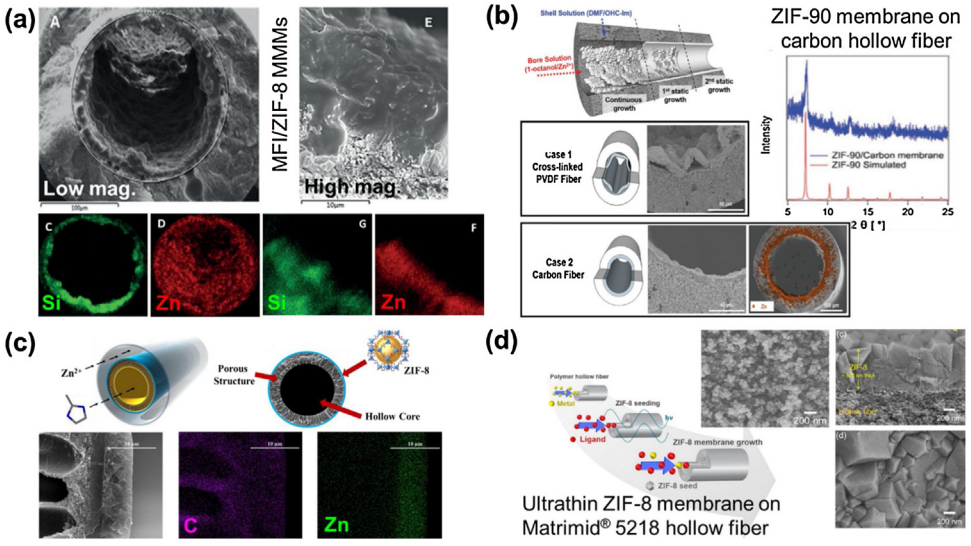

Fig. 6. Interfacial synthesis strategy to prepare (a) all nanoporous MFI/ZIF-8 MMMs on Torlon® hollow fibers (b) ZIF-90 membranes on macroporous carbon hollow fibers. Continuous microfluidic flow processing strategy to prepare ZIF-8 membranes on (c) Torlon® hollow fibers via in-situ growth and (d) Matrimid® 5218 hollow fibers via secondary growth. Reproduced with permission from Ref. [136] Copyright 2019 Wiley VCH, Ref. [86] Copyright 2017 Wiley VCH, Ref. [139] Copyright 2017 American Chemical Society, and Ref. [117] Copyright 2018 Elsevier B.V.

circumstance, the use of polymeric substrates is not recommended as most of them have poor chemical stability in these solvents. In an attempt to grow ZIF-90 membranes on cross-linked PVDF hollow fibers, Eum et al. [86] observed detachment/delamination of ZIF-90 films from the PVDF substrates (Fig. 6(b)). Swelling of the hollow fibers in dimetylformamide and later contraction to its original dimension upon drying created interfacial strains to the ZIF-90 layer which led to detachment and crumpling of the layer. Replacing PVDF hollow fibers with 'inert' carbon hollow fibers eliminated the swelling issues, resulting in defect-free ZIF-90 membranes with thickness of 3.1 μm.

Continuous microfluidic flow processing

Continuous microfluidic flow processing has become an increasingly popular method to synthesize ZIF membranes especially on bore space of hollow fibers. Polycrystalline ZIF-7, ZIF-8, ZIF-90, and ZIF-93 membranes have been successfully fabricated using this strategy [88,100,115,117,139,141,142]. In a typical synthesis, ZIF precursors are continuously fed through bore or shell side of hollow fibers (using peristaltic or syringe pumps) for a predetermined period to obtain defect-free membranes. In most cases, the synthesis is performed under room temperature conditions. Membrane grown on bore of hollow fibers uses a relatively small amount of precursor solution (due to small bore space of the fibers), contributing to cost saving.

Several flow protocols have been developed to prepare ZIF membranes on hollow fibers. Cacho-Bailo et al. [142] continuously injected a mixture of metal and linker precursors to bore space of polysulfone hollow fibers (inner diameter, ID 315 μm) at a flow rate of 100 $\mu L\,min^{-1}$ for 75 min to in-situ form ZIF-7 and ZIF-8 membranes. The prepared ZIF-8 (3.6 μm thick) and ZIF-7 (2.7 μm thick) membranes were then tested for H_2 purification and CO_2 separations. In another work, Marti et al. [139] separately injected 2-methylimidazole and Zn precursor solutions through shell and bore side of Torlon® hollow fibers (outer diameter, OD 400 μm), respectively, to prepare ZIF-8 membranes on the hollow fibers (Fig. 6(c)). The ~8.8 μm thick ZIF-8 membranes were then tested post-combustion CO_2 capture application. The locations of ZIF-8 layers on the hollow fibers were manipulated by simply switching the flow of precursor solutions from the shell side to the bore side and vice versa.

Jeong et al. [115–117] and Huang et al. [100] utilized continuous microfluidic secondary growth to grow ZIF-8 seed layers on bore of polymer (e.g., Matrimid® 5218, ID 344 μm and PVDF, ID 1400 μm) and α-Al_2O_3 (ID 1000 μm) hollow fibers previously obtained via solvothermal or microwave heating. In both studies, Zn and 2-methylimidazole precursors were first mixed and aged for several minutes. The growth solution was then fed through the bore space of the hollow fibers at a specified flow rate/duration to allow the seed crystals to grow and form coherent films (Fig. 6(d)). One advantage of this approach is flexibility to choose duration of secondary growth and flow rate of growth solution, which enables a formation of thinner ZIF membranes. Continuous and well-intergrown ZIF-8 membranes as thin as ~800 nm thick on bore side of Matrimid® 5218 hollow fibers were demonstrated by our group [117]. It is important to note that during synthesis, bulk crystallization of ZIFs still exists [143]. That is to say, if these homogenously grown ZIFs were not utilized for example as adsorbents, it will lead to a waste of expensive precursors.

Solvent-free vapor phase synthesis

Another innovative route to prepare ZIF membranes on porous supports is via solvent-free crystallization. A solvent-free vapor phase synthesis is able to produce high flux and high selectivity membranes. To the best of our knowledge, the thinnest ZIF membranes (~17 nm thick) reported to date are prepared using this method. The method is fairly simple, therefore amenable for scale up. In a typical process, metal precursors such as metal-based gel and metal oxides are deposited on substrates via dip-coating [130], electrodeposition [144], atomic layer deposition [79], etc. The metal precursors are then exposed to a ligand vapor environment to convert the metal precursors into ZIFs. An important factor to consider in this process is obtaining high ligand vapor concentrations without significant decomposition of the ligands [145]. Therefore, the ability of solid ligands to be vaporized without them being decomposed may limit the choice of

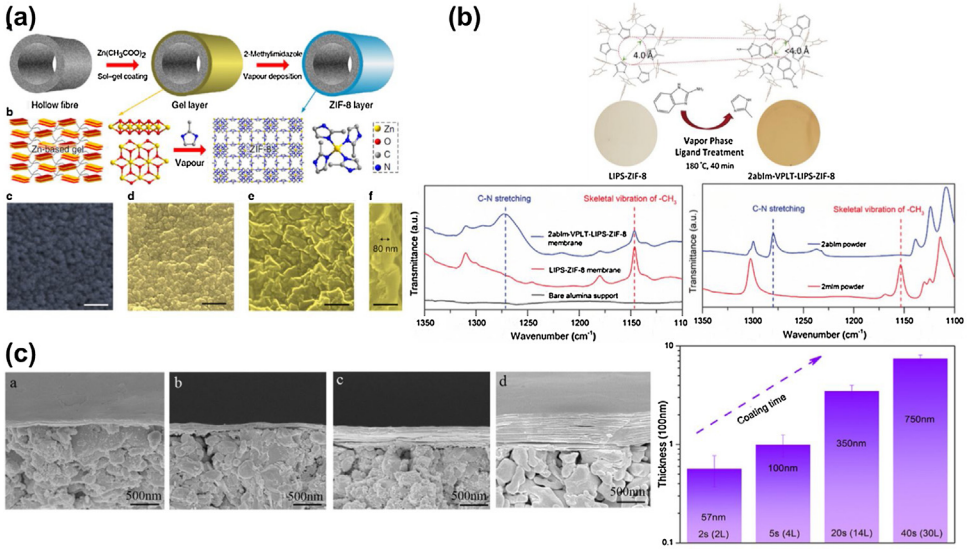

Fig. 7. Vapor phase strategy to synthesize ultrathin ZIF-8 and hybrid ZIF membranes on porous supports. (a) Zn gel layer on PVDF hollow fiber is transformed into ZIF-8 membranes under mIm ligand vapor environment. (b) ZnO layer on α-Al_2O_3 disc is subjected to mIm vapor environment to form ZIF-8 membranes. Subsequent vapor phase 2abIm ligand treatment led to incorporation of the ligands into parent ZIF-8 frameworks. (c) Scanning electron micrograph of various Co-based ZIF membranes prepared via vapor phase transformation. Reproduced with permission from Ref. [130] Copyright 2017 Springer Nature, Ref. [147] Copyright 2019 John Wiley and Sons and Ref. [146] Copyright 2018 Elsevier B.V.

linkers, hence, ZIF materials that can be fabricated into membranes. A beneficial aspect of solvent-free crystallization is the use of large volume of solvent during synthesis is eliminated which makes it an environmentally friendly method.

Li et al. [130] fabricated ultrathin ZIF-8 membranes on the shell side of PVDF hollow fibers for C_3H_6/C_3H_8 separations using a gel-vapor transformation. As shown in Fig. 7(a), thin layers of Zn gel were coated on the shell side of the hollow fibers. The hollow fibers were then exposed to 2-methylimidazole (mIm) vapor at 150 °C for several hours to complete the crystallization process. Regulating Zn gel concentration and coating time were critical to obtain continuous gel layer with different thicknesses. As a result, ultrathin ZIF-8 membranes with thicknesses ranging from 17 nm to 757 nm were prepared. Nian et al. [146] on the other hand synthesized Co-based ZIF ($Co_2(bIm)_4$, bIm - benzimidazole) membranes on the bore side of ceramic tubular supports for H_2/CO_2 separations. Unlike Li's work [130] mentioned above, Nian's work involves an intermediate step where the metal gel layer was first heat treated to convert the Co gel to Co_3O_4 before exposing it to bIm vapor. It is important to point out that the use of solid-state metal precursors to prepare ultrathin membranes using metal gel transformation can be quite challenging due to high viscosity of the gel.

Ma et al. [79] introduced a liquid/gel-free ligand-induced permselectivation (LIPS) method to prepare high performance ZIF-8 membranes for C_3H_6/C_3H_8 separations. Atomic layer deposition (ALD) was used to obtain zinc oxide (ZnO) deposits on top and inside γ-alumina layer. The ALD cycles were repeated up to 50 cycles to form an impermeable ZnO barrier on the supports. The ZnO layer was then transformed into a selective and permeable ZIF-8 barrier under mIm ligand vapor environment. C_3H_6/C_3H_8 separation performances of the membranes were among the best that have been reported for ZIF-8 and ZIF-67 membranes. Following this, they performed vapor phase ligand exchange (VPLT) of 2-aminobenzimidazole (2abIm) to partially exchange the mIm ligands of ZIF-8 [147]. As depicted in Fig. 7(b), incorporation of bulkier 2abIm ligands reduces ZIF-8 effective pore sizes thereby shifting the molecular cut-off towards smaller molecules (e.g., CO_2, O_2, N_2, and CH_4). The emergence of new broad IR peaks at 1280 cm^{-1} confirms the incorporation of 2abIm ligand into VPLT-LIPS-ZIF-8 membranes. The vapor phase concept has also been extended to allow permselectivity tuning of ZIF-8 membranes. In their most recent work, Hayashi et al. [148] performed a facile vapor phase treatment of ZIF-8 membranes with manganese (II) acetylacetonate ($Mn(acac)_2$). The membrane selectivity dramatically increased due to a presence of $Mn(acac)_2$ deposits on the surface of the membranes.

A key benefit of ALD is ability to deposit a uniform and conformal thin film on substrates with angstrom level precision [149,150]. While ALD has many desirable features, ALD is a slow process with low deposition rates. For example, the growth rate of ZnO on various substrates by ALD is in the range of 0.5–4.0 Å $cycle^{-1}$ [151]. Moreover, ALD is an energy-intensive process that generates a high rate of waste [149]. Nonetheless, the proposed all-vapor ZIF-8 membrane synthesis above-mentioned is groundbreaking and has the potential to effectively suppress several challenges that conventional solution-based membrane synthesis currently facing.

Electrochemical based synthesis

Electrochemical deposition is one of the promising and industrially relevant methods to in-situ form MOF/ZIF thin films and membranes. Zhang et al. [152] provided a comprehensive review of MOF deposition via electrochemical deposition. Electrochemical deposition of MOF/ZIFs on substrates can be categorized into three types: (i) electrophoretic deposition, (ii) anodic deposition, and (iii) cathodic deposition [152].

Electrophoretic deposition technique uses an external electric field to mobilize charged nuclei present in the bulk solution to substrates positioned at the oppositely charged electrode [152]. The flux of the nuclei driven to the substrates is proportional to the electric field strength, nuclei concentration in the solution, and electrophoretic mobility [153]. The deposited ZIF nuclei on the substrates, if necessary, can be subjected to further crystal growth to promote better film intergrowth. He et al. [127] introduced a novel electrophoretic nuclei assembly for crystallization of highly intergrown thin films technique (ENACT) to prepare ultrathin and defect-free ZIF-7 and ZIF-8 membranes on AAO discs for H_2 purifications and C_3H_6/C_3H_8 separations. In ENACT, ZIF sols were first aged for a few minutes (>3 min). Then, a constant electric field was applied for up to 4 min to mobilize the ZIF nuclei to the substrates. The substrates were then left inside the synthesis sol at constant temperature for 2 h to promote further crystals growth, thereby forming continuous and well-intergrown membranes. The reported ZIF-7 and ZIF-8 membrane thicknesses were ~2.7 μm and ~0.5 μm, respectively. Synthesis of ZIF membranes on various porous substrates including ceramic, copper foil, carbon, and polyacrylonitrile using ENACT were also reported. An advantage of ENACT is the substrates do not necessarily have to be conductive or require any surface modifications to deposit ZIF crystals. ENACT also is a facile and rapid method which holds merit for scale up.

Anodic deposition technique uses a metal anode to supply the building block of ZIFs (metal ions) to the synthesis solution through anodic dissolution of the anode [154,155]. The metal ions then interact with linkers in the electrolyte solution to form ZIF crystals on substrates. In cathodic deposition, both metal ions and linkers are present in the solvent. Electrochemical reduction of a probase near the cathodic electrode region generates base, which goes on to increase local pH of the solution [156]. A high pH environment at the vicinity of the electrode facilitates deprotonation of neutral linkers, inducing ZIF nucleation and growth on the substrates [128]. One drawback associated with the above-mentioned techniques (i.e., anodic and cathodic deposition) is they both require conductive surfaces to attract metal ions to the cathode side and to promote deprotonation of linkers. Commonly used non-conducting substrates such as ceramic or polymer need to be rendered conductive (by coating them with a conductive layer) for the method to work.

To the best of our recollection, all ZIF membranes (i.e., ZIF-7, ZIF-7-8, ZIF-8, and Co–Zn–ZIF-8) for separation applications reported in literature were synthesized via cathodic deposition. The only work that reports on ZIF thin film formation via anodic deposition was by Worrall et al. [157]. Worrall et al. [157] deposited a variety of ZIF thin films including ZIF-4, ZIF-7, ZIF-8, ZIF-14, and ZIF-67 on Cu or Zn foil for supercapacitor applications. Zhou et al. [133] developed fast current-driven synthesis (FCDS) that enabled formation of ultrathin ZIF-8 membranes for C_3H_6/C_3H_8 separations. The membranes were synthesized in-situ inside an electrochemical cell containing methanolic solution of Zn(COOH), 2-methylimidazolate (mIm), and $(NBu_4)PF_6$ modulator. 200 nm thick ZIF-8 membranes on AAO discs were prepared in just under 20 min. ZIF-8 thin films on stainless steel nets, Ni foam, and porous stainless steel discs were also demonstrated. Exposure to external direct current generated ZIF-8 membranes with a newly discovered ZIF-8_Cm phase with more suppressed linker mobility compared to the normal ZIF-8_I43 m phase. Stiffer ZIF-8_Cm frameworks of the synthesized membranes resulted in a superior C_3H_6/C_3H_8 molecular sieving capability. In their follow up work, they synthesized mixed-linker ZIF-7-8 membranes on AAO discs using a similar FCDS technique showing unprecedented CO_2/CH_4 separation performances [94]. In this case, a combination of

frameworks stiffening and pore narrowing from the addition of bulky secondary benzimidazole (bIm) ligands sharpened CO_2/CH_4 sieving properties of the membrane. Most recently, they fabricated a series of bimetallic (Co_{100-x}–Zn_x–ZIF-8) with thickness of less than 700 nm in just under 20 min [46]. The AAO discs were immersed in a synthesis solution (a mixture of Zn and Co salt in methanol with a total metal concentration of 0.1 M and mIm in methanol with a concentration of 0.2 M) which were then subjected to a current density of 0.7 mA cm^{-2} at room temperature for several minutes.

Wei et al. [128] used aqueous cathodic deposition (ACD) method to synthesize ZIF-8 membranes on AAO discs for C_3H_6/C_3H_8 separations. The method used 100% water as solvent and did not require addition of modulators. In setup shown in Fig. 8(a), a conductive AAO disc was used as a cathodic electrode while graphite paper was used as an anodic electrode. The AAO disc was coated with platinum/palladium via sputtering to enhance disc electrical conductivity. An optimal current density of 0.13 mA cm^{-2} was chosen to prevent excessive water electrolysis and to obtain high ZIF crystal deposition rates. High mIm to Zn ratio (Zn:mIm ratio of 1:60) and dilute Zn solution (Zn:H_2O of 1:3889) were used to ensure complete linker deprotonation and to slow down crystal growth in the bulk solution, respectively. Fig. 8(b) shows the evolution of film morphologies from 10 min to 60 min. Longer synthesis time resulted in thicker ZIF-8 membranes with larger grain sizes. Among ZIF-8 membranes that were synthesized, the 500 nm thick ZIF-8 membranes displayed the highest C_3H_6/C_3H_8 separation factor, outperforming the majority of reported ZIF-8 membranes for C_3H_6/C_3H_8 separations.

From our observation, ENACT, FCDS, and ACD able to produce ZIF-8 membranes with thickness of less than 500 nm. Despite having thin membranes, C_3H_6/C_3H_8 selectivity of the membranes are still greater than 100, indicating that the membranes possess better microstructures and fewer defects. Short synthesis time and gap-filling mechanism of the exposed substrates are the likely reason behind this. ZIF-8 is non-conductive. Once the crystals form and cover support conductive surfaces, they act as insulating layers that prevents further crystals growth [133]. There will be fewer crystal formation on top of the already formed crystals and 'piling up' of crystals are suppressed, forming single monolayer thick membranes [158]. Moreover, rapid membrane synthesis time provides a narrow window for crystal growth.

At this moment, electrochemical-based membrane synthesis only focuses on mechanically weak AAO flat substrates which limit the gas permeation measurement pressure to 2.0 bar only [128]. For practical applications, it is beneficial to demonstrate the applicability of the FCDS and ACD to grow ZIF membranes on stronger substrates such as α-Al_2O_3 discs or metal plates which are able to tolerate higher transmembrane pressure difference (e.g., typical pressure for C_3H_6/C_3H_8 separation is around 18 atm) [159]. Also, the substrates need to be rendered conductive for the FCDS and ACD technique to work but one has to admit that it is difficult to render nonconductive polymer or ceramic to be conductive [133]. Electrochemical-based synthesis have the potential to prepare ZIF membranes on high surface-to-volume substrates as membrane formation is believed to be less sensitive to substrate geometry but there are no successful demonstration reported. Electrochemical deposition method definitely has the potential to produce ultrathin and high performance ZIF membrane for commercial applications, but further substantial research effort is required.

Application areas of ZIF membranes

Applications of membrane technology in industrial gas separations are somewhat limited where the majority of installed membrane modules, mostly polymers, are used in only four common applications: (i) H_2 recovery – H_2/N_2, H_2/CH_4, etc. (ii) N_2 production from air – N_2/O_2 (iii) natural gas treatment – H_2S/CH_4, CO_2/CH_4, etc. (iv) vapor recovery – C_2H_4/N_2, C_3H_6/N_2, etc. [6,10]. In gas separation membranes, finding candidate materials with proper transport properties is critical to ensure high product purity and recovery rate. The majority of ZIFs, especially SOD-type ZIFs have apertures in the size range of important gases, therefore could be used as membrane materials for gas separations. Preparation of ZIF membranes for gas separations has been an active research area in the past decades. There has been a number of excellent reviews on ZIF polycrystalline membranes available in literature to keep the reader updated with the recent progress in the area [49–54].

In this section, we review three unsolved membrane applications that, if sorted out, might disrupt the current gas separation market that mostly dominated by conventional technologies (e.g., distillation, adsorption, and absorption). Unsolved application areas that will be discussed in this section are H_2 purification (H_2/CO_2), CO_2 separations (CO_2/N_2 and CO_2/CH_4), and condensable gas separations (C_2H_4/C_2H_6, C_3H_6/C_3H_8, and n-C_4H_{10}/i-C_4H_{10}). In this section, we first present benchmark transport properties required for the membranes to be competitive with the existing technologies. Then, we review majority of the examples of ZIF-based membranes for gas separations that are currently available. The gas

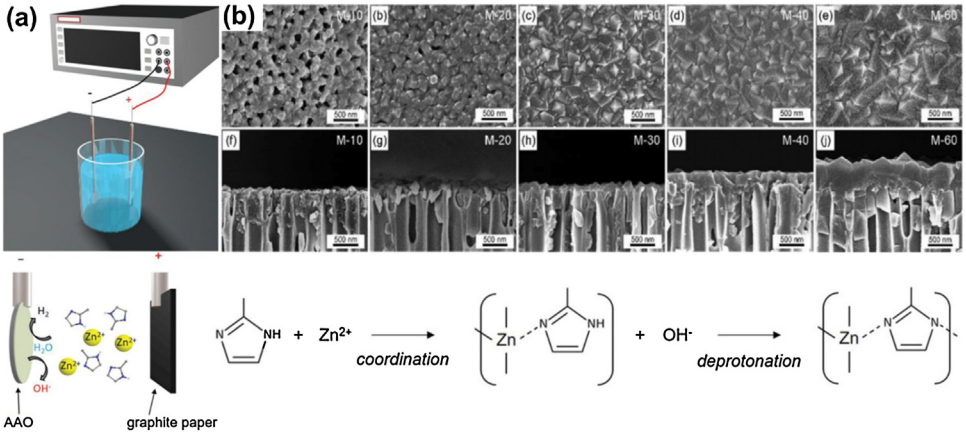

Fig. 8. (a) Synthesis of ultrathin ZIF-8 membrane using aqueous cathodic deposition. (b) Morphological evolution of ZIF-8 membranes synthesized using method shown in (a) at 10 min, 20 min, 30 min, 40 min, and 60 min synthesis time. Reproduced with permission from Ref. [128] Copyright 2019 John Wiley and Sons.

separation performances of the membranes are summarized in a form of table or pseudo-Robeson plot (permeance vs. selectivity).

H_2 purifications

H_2 is considered as a clean, efficient, and sustainable energy carrier with zero greenhouse gas emission and no environmental damage (oxidization of H_2 produces only water vapor). High purity H_2 is used in several important industrial applications including petroleum refining, aerospace applications, ammonia production, glass purification, semiconductor manufacturing, etc. [160]. Like any other important gases, H_2 coexists along with other components (e.g., N_2, CO, CO_2, and CH_4) during chemical processes, thereby requiring its separation [9]. Large capital investments are required for the installation of conventional separation technology to isolate H_2 from less desirable species, which consequently drives the overall H_2 cost up [161]. Efficient purification and recovery of H_2 requires a state-of-the-art separation technology and membrane technology is expected to play a key role in a cheaper production of H_2.

From a historical perspective, the very first commercial polymer-based hollow fiber membranes for H_2 separations, namely PRISM® membranes, were developed by Monsanto (part of Air Products and Chemicals Inc.) in the late 1970s. PRISM® membranes (polysulfone) were originally designed to separate H_2 from N_2 from ammonia reactor purge streams but later expanded for wider applications including H_2/CO syngas ratio adjustment and H_2 recovery from hydrocarbon and/or hydrotreater off-gas streams [18]. Following the commercial success of PRISM® membranes, cellulose acetate spiral-wound membranes (Separex, part of Honeywell UOP) and polyimide membranes (Ube Industries) were developed for similar applications [18,161–163]. Membrane-based gas separation has expanded since then and new membrane materials were developed for other applications such as CO_2 separation from natural gas. According to Galizia et al. [10], H_2 separations (i.e., H_2/N_2, H_2/CO, and H_2/CH_4) were considered as solved problem in gas separation membranes. Considering the large scale success of polymer membranes for H_2 separations, there is little interest to develop more H_2-selective membranes for the above-mentioned applications.

ZIF membranes have the opportunity to be utilized for emerging applications of H_2 separations particularly for H_2/CO_2 separations. The most common routes of producing H_2 are through hydrocarbon reforming and coal gasification, producing roughly 96% of the global H_2 supply [164]. The remaining fraction is produced through water electrolysis [161]. The production of H_2 via steam methane reforming begins with initial reforming step reactions at 820 °C (2) [161,165]. Additional H_2 is obtained through water-gas-shift (3) and steam methane reforming reactions (4).

$$CH_4 + H_2O \rightarrow CO + 3H_2 \quad (2)$$

$$CO + H_2O \rightarrow CO_2 + H_2 \quad (3)$$

$$CH_4 + 2H_2O \rightarrow CO_2 + 4H_2 \quad (4)$$

The resulting mixtures consist of 74% H_2 and 18% CO_2 which requires a CO_2 removal process to obtain high purity H_2 [161]. Membrane technology is not widely explored for H_2/CO_2 separation due to low gas selectivity. As compiled by Robeson, the majority of reported polymer membranes have H_2/CO_2 selectivity of less than 10 [13]. Galizia et al. [10] argue that the required properties for commercially attractive H_2/CO_2 separation membranes are H_2 permeance greater than 200 GPU and H_2/CO_2 selectivity greater than 10. For this application, polycrystalline ZIF membranes might have the potential to be utilized. There is no shortage of scientific works on ZIF membranes with promising H_2/CO_2 separation performances. H_2/CO_2 separation performances of the recently reported ZIF membranes are presented in Table 1. Additionally, H_2/N_2 and H_2/CH_4 separation performances of the membranes are also included.

ZIF-8 is one of the most widely investigated ZIFs for H_2 separations. Generally speaking, polycrystalline ZIF-8 membranes are not effective to isolate H_2 from CO_2 due to lattice flexibility. As illustrated in Fig. 9, H_2 permeance through ZIF-8 membranes is unprecedentedly high, reaching a value of 24,641 GPU. Gas permeances through the membranes decreases following the order of molecule kinetic diameters: H_2 (2.9 Å) > CO_2 (3.3 Å) > N_2 (3.6 Å) > CH_4 (3.8 Å). The reported H_2/CO_2 selectivity of the membrane is higher than the Knudsen selectivity (7.0 vs 4.7), but fall short of the commercial requirements. In another work, ultrathin ZIF-8 membranes supported on PVDF hollow fibers prepared by Li et al. [130] showed high H_2 permeance of 10,454 GPU but low H_2/CO_2 ideal selectivity of 7.3. Despite showing impressively high H_2 permeances in the order of several thousand GPUs, H_2/CO_2 selectivities of ZIF-8 membranes were unattractive (see Table 1). H_2/CO_2 selectivity of ZIF-67 (Co-substituted ZIF-8) membranes is slightly higher than those of ZIF-8 membranes due to stiffer Co–N bonding, but still not attractive enough for commercial applications. At 25 °C and 1 bar feed pressure, ZIF-67 membranes by Zhou et al. [166] displayed H_2 permeance of 4933 GPU and ideal H_2/CO_2 selectivity of 17.

Among ZIFs that are available, ZIF-7 might be better suited for H_2/CO_2 separations due to its narrower apertures (3.0 Å) than ZIF-8. ZIF-7 is constructed by linking benzimidazoles with Zn ions forming a cubic SOD zeolite topology [37]. Unlike ZIF-8 membranes that can be easily prepared using simple solvents (e.g., methanol or water), ZIF-7 membranes are synthesized under solvothermal conditions using dimethylformamide (DMF) as a solvent [80,98,112,167]. ZIF-7 membrane activation can be tricky as DMF removal from ZIF-7 cavities may lead to phase transition from ZIF-7-I to a highly-distorted and locally-strained ZIF-7-II or layered and non-porous structure of ZIF-7-III phase [168]. As shown in Table 1, the majority of the reported ZIF-7 membranes have higher H_2/CO_2 selectivity than those of ZIF-8. Increasing permeation temperature improves separation efficiency as H_2 transport through the membranes is less affected by temperature compared to CO_2. Kim and Lee [169] observed H_2/CO_2 separation factor of their ZIF-7 membranes increased to 10 when measurement temperature was increased to 150 °C. Selectivity increase with temperature is beneficial considering the potential application of the membrane which is high temperature separation of H_2 from CO_2 output of WGS reactor [170].

ZIF-95 with POZ topology has a narrow aperture of 3.7 Å estimated from single-crystal structure data and has strong affinity toward CO_2 due to quadrupolar interaction between CO_2 and ZIF-95 linkers [36,89]. Strong adsorption between CO_2 and ZIF-95 framework limits the CO_2 diffusion mobility through the framework. Ma et al. [172] synthesized ZIF-95 membranes on porous α-Al_2O_3 discs via a seeded growth. The membranes showed high H_2 permeance of 507 GPU and H_2/CO_2 selectivity of 42. In their follow up work, they synthesized *c*-oriented ZIF-95 membranes by secondarily growing the ZIF-95 nano-sheet seed layers using vapor-assisted in-plane epitaxial growth [171]. Gas permeances through the membrane decreased following the order of molecular kinetic diameter as depicted in Fig. 10(a). At 50 °C and 1 bar, the secondarily grown ZIF-95 membranes displayed H_2 single gas permeance and H_2/CO_2 ideal selectivity of 1633 GPU and 29, respectively. H_2 permeance and H_2/CO_2 ideal selectivity increased to 2882 GPU and 39, respectively, upon increasing permeation temperature to 225 °C as shown in Fig. 10(b). Meanwhile, 50 μm

Table 1
Single and/or mixed gas permeances and selectivities of various ZIF membranes for H_2 purifications.

ZIFs	Substrates	Synthesis method	Thickness (μm)	H_2 permeance (GPU)	Selectivity			Test conditions	Ref.
					H_2/CO_2	H_2/N_2	H_2/CH_4		
ZIF-7	PVDF hollow fiber	Solvothermal synthesis	30	3,969	16.3	18.3	–	RT	[98]
ZIF-7	Polysulfone hollow fiber	Microfluidic synthesis	2.4	6	2.4	35.1	34.6	1 bar Single gas 35 °C	[142]
ZIF-7	Polypropylene flat sheet	Chelation assisted in-situ growth	28	14,575	10.6	–	–	TMP: 0–3 bar Mixed gas (1:1) 35 °C	[167]
ZIF-7	α-Al_2O_3 disc	Secondary growth	17	299	19	–	–	1 bar Single gas RT – 120 °C (RT*) 1–2 bar (1*)	[112]
ZIF-8	PVDF hollow fiber	Solvothermal synthesis	46	7,297	12.2	14.3	–	Mixed gas (1:1) RT	[98]
ZIF-8	Polysulfone hollow fiber	Microfluidic synthesis	3.6	14	2.6	18.3	17.2	1 bar Single gas 35 °C	[142]
ZIF-8	PVDF hollow fiber	Continuous flow (secondary growth)	1.2	4,878	6.0	10.2	12.1	TMP: 0–3 bar Mixed gas (1:1) RT	[116]
ZIF-8	Al_2O_3–ZnO hollow fiber	Solvothermal synthesis of functionalized substrates	5.0	5,406	–	12.6	12.9	1 bar Single gas N/A	[176]
ZIF-8	PES hollow fiber	Zn gel transformation	20	3,285	5.2	22.7	–	1 bar Single/mixed* gas 20 °C	[177]
ZIF-8	γ-Al_2O_3 tube	Partial self-transformation of LDH	1.1	122	–	16.8	54.1	1 bar Single gas 90–150 °C (90*)	[178]
ZIF-8	AAO disc	ENACT	0.5	24,641	7.3	15.5	16.2	1 bar Single gas 25 °C	[127]
ZIF-8	PVDF hollow fiber	Direct immersion in synthesis solution	1.0	60,035	7.0	7.8	8.6	1 bar Single gas 20 °C	[97]
ZIF-8	PVDF hollow fiber	Direct immersion in synthesis solution	1.1	27,747	7.4	6.4	5.3	1–10 bar (1*) Single gas 20 °C	[175]
ZIF-8	BPPO flat sheet	Chemical vapor modification of substrate	0.2	6123	12.8	9.7	–	1–10 bar (1*) Single gas 25 °C	[131]
ZIF-8	α-Al_2O_3 disc	LbL deposition followed by solvent free crystallization	7.0	2,001	12.3	7.5	8.7	1 bar Single gas 25 °C	[68]
ZIF-9	α-Al_2O_3 tube	Heteroepitaxial growth from ZnO nanorod	10	552	23.8	8.9	7.6	1 bar Mixture gas 25–150 °C (25*)	[173]
ZIF-9	α-Al_2O_3 tube	In-situ growth of APTES functionalized substrates	4.0	552	24.2	8.8	16.7	1 bar Single gas 25 °C	[82]

Table 1 (*Continued*)

ZIFs	Substrates	Synthesis method	Thickness (μm)	H_2 permeance (GPU)	Selectivity			Test conditions	Ref.
					H_2/CO_2	H_2/N_2	H_2/CH_4		
ZIF-67	α-Al_2O_3 tube	Heteroepitaxy growth from ZnO nanorods	3.0	657	8.6	21.8	45.4	1 bar Single*/mixed gas 25–150 °C (25*)	[173]
ZIF-67	α-Al_2O_3 tube	Solvothermal conversion of ZnO nanorods	5.0	245	11.6	28.7	33.1	1 bar Single gas 30 °C	[179]
ZIF-67	α-Al_2O_3 tube	Solvothermal conversion of cobalt nanowires	2.0	1,668	–	14.7	15.3	1 bar Mixed gas (1:1) 30–150 °C (30*)	[180]
ZIF-67	α-Al_2O_3 disc	Self-conversion of cobalt layer	3.0	4,933	16.8	16.5	18.0	1 bar Single gas 25 °C	[166]
ZIF-90	α-Al_2O_3 disc	Solvothermal synthesis APTES functionalization	20	851	21	–	77	1 bar Single*/mixed gas 25–225 °C (225*)	[87]
ZIF-93	P84 co-polyimide hollow fiber	Microfluidic synthesis	3.0	10	–	–	60	1 bar Single gas 35–100 °C (35*)	[88]
ZIF-95	α-Al_2O_3 disc	Solvothermal secondary growth	20	507	41.6	36.8	40.3	1.25 bar Mixed gas (1:1) 200 °C	[172]
ZIF-95	α-Al_2O_3 disc	Vapor-assisted in plane epitaxial growth	0.6	2,882	38.5	–	64.3	1 bar Mixed gas (1:1) 100 °C	[171]
ZIF-100	α-Al_2O_3 disc	Solvothermal growth on modified support	50	188	77	25	46	1 bar Single*/mixed gas 25 - 150 °C (25*) 1–4 bar (1*)	[90]

1 GPU = 3.348×10^{-10} mol m^{-2} s^{-1} Pa^{-1}.
* Measurement conditions used of the reported H_2 permeance and H_2/CO_2, H_2/N_2, and H_2/CH_4 selectivity.

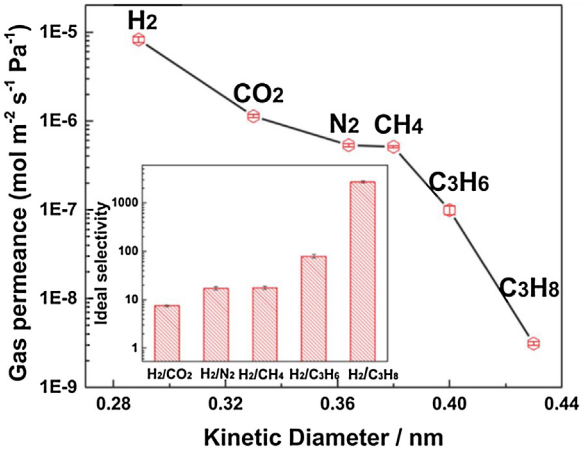

Fig. 9. Single gas permeances and ideal selectivities of various gases through ZIF-8 membranes. Permeation measurements were performed at room temperature and atmospheric pressure. Reprinted with permission from Ref. [127] Copyright 2018 Wiley VCH.

thick ZIF-100 membranes (ZIF-100 has MOZ cage and aperture of 3.35 Å) solvothermally grown on modified α-Al_2O_3 discs displayed H_2 permeance and H_2/CO_2 selectivity of 188 GPU and 77, respectively [36,90]. Other ZIFs such as ZIF-9 [82,173], ZIF-90 [87], and ZIF-93 [88] have also been synthesized and tested for H_2 purifications. Huang's et al. [87] reported ZIF-90 membranes with H_2 permeance of 845 GPU and H_2/CO_2 ideal selectivity of 21 measured at a temperature of 225 °C. Despite having wider effective apertures of 5.0 Å, interestingly enough, ZIF-90 membranes still maintain high H_2/CO_2 selectivity attributable to the pore narrowing from the APTES modification [87]. Moreover, strong interactions between CO_2 and carbonyl group (C=O) of ZIF-90 linkers slow down the CO_2 diffusion through the lattice relative to H_2 [174].

While there are many promising ZIF membranes with commercially attractive performances (i.e., H_2 permeance > 200 GPU and H_2/CO_2 selectivity > 10), there is still growing concern about long term stabilities and separation performances of the membranes at elevated temperature [18]. ZIF-8 membranes on PVDF hollow fibers prepared by Hou's et al. [97] showed stable performances over a period of 30 days at room temperature

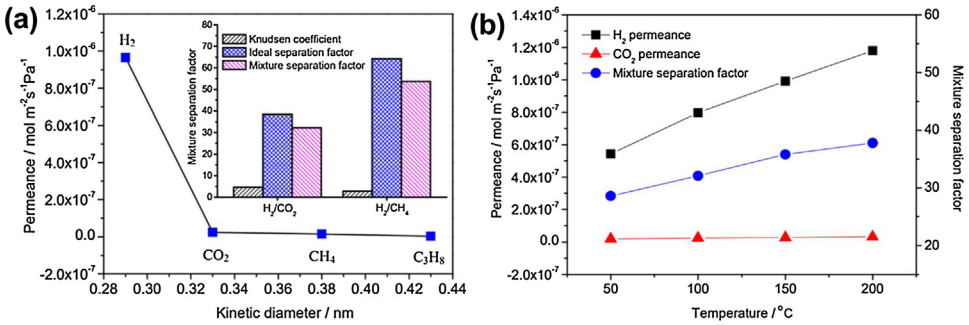

Fig. 10. (a) Single gas permeances and ideal selectivities of various gases through ZIF-95 membranes at 100 °C and 1 bar. (b) H_2/CO_2 binary gas permeances and separation factor of ZIF-95 membranes as a function of temperature at pressure of 1 bar. Reprinted with permission from Ref. [171] Copyright 2020 Wiley VCH.

conditions. However, after subjecting the membrane to a high temperature of 120 °C for 48 h, they observed H_2 permeance dropped by 71%. They concluded that the prepared ZIF-8 membranes were not suitable for prolonged high temperature separations due to loss of crystalline structures of ZIF-8 [97]. Stability of ZIF membranes under humid condition is another important criteria that needs to be evaluated considering that the outputs of WGS reactors contain a significant amount of water vapor. Hydrothermal stability test performed by Kim and Lee [169] revealed that ZIF-7 membranes were not stable under humid conditions. After hydrothermal treatment (20% water vapor in the gas stream) at 300 °C for 24 h, they observed a formation of large cracks/voids and considerable decomposition of ZIF-7 crystals. Also, there is a lack of high pressure testing of the prepared ZIF membranes. The highest upstream pressure tested for H_2/CO_2 measurements was at pressure of 10 bar by Hou et al. [175]. They observed ~3% and ~10% reduction in H_2 permeance and H_2/CO_2 separation factor, respectively, upon increasing feed gas pressure to 10 bar.

CO_2 separations

Overreliance on the burning of fossil fuels to keep up with the energy needs from the rapidly expanding modern society has led to a surge in CO_2 emission to the earth atmosphere. In the United States, the nation's total CO_2 emission grew to 6.022×10^9 metric tons in 2007 and the figure represents more than 80% of the nation's total greenhouse gas emission [14,181,182]. As a major component of greenhouse gases, there is a growing concern that continuous and unregulated release of CO_2 to the atmosphere might trigger serious global warming issues. Carbon capture and storage are considered as the most promising solution to ramp down the emission of the greenhouse gases [183,184]. Currently, amine-based absorption technology is the most mature technology for CO_2 removal, representing 90% of the total market share [185]. However, drawbacks of this process are high capital cost and energy penalty of solvent regeneration [184,186]. Also, operational complexity of the process requires regular maintenance and full-time supervisions [11].

Membrane-based technology is considered as a promising and environmentally friendly alternative compared to the conventional amine-based technology for CO_2 separations [14,187–189]. Separations of CO_2 from the flue gas from chemical/power plants using membrane technology are challenging for a number of reasons. Firstly, flue gases contain low concentration of CO_2 (10–16 wt%) and available only at atmospheric pressure providing insufficient driving force for permeation unless compression is applied [185,190]. Secondly, ppm level impurities (e.g., SO_x and NO_x) and water vapor in the flue gases tend to reduce the separation efficiency of the membranes. It is estimated that a rational pressure ratio for membrane system for post-combustion CO_2 capture applications is between 5 and 10, above which the entire process becomes economically unaffordable [14,191]. Pressure ratio limited separation coupled with the sheer amount of flue gases to be treated mean that the membrane system requires large membrane area to perform the intended separations. Under these circumstances, highly productive membranes are desirable to cut down the required membrane area to retain market attractiveness.

For CO_2 capture from flue gas, commercially attractive membranes are expected to have CO_2 permeance and CO_2/N_2 separation factor in the range of 1,000–5,000 GPU and 30–50, respectively [10]. Meanwhile, for large scale CO_2 removal from natural gas (i.e., CO_2/CH_4 separations), the target CO_2 permeance and CO_2/CH_4 separation factor for the membrane are >100 GPU and 20–30, respectively [10]. CO_2/N_2 separations are considered as unsolved applications in membrane industries. Membranes for CO_2/CH_4 separations on the other hand have already been commercialized (currently occupies 10% of the market share for CO_2 removal from natural gas) [10]. However, there is an urgency to develop better-performing membranes to make the current two-stage CO_2/CH_4 membrane design as competitive as the amine absorption technology [18].

ZIF-8 membranes do not possess attractive separation properties for CO_2/N_2 and CO_2/CH_4 mixtures. Unlike zeolites with rigid frameworks, ZIF-8 framework is rather flexible, providing at best, moderate CO_2/N_2 and CO_2/CH_4 molecular sieving effects [39]. Single crystal ZIF-8 membrane measurements showed that ZIF-8 has promisingly high intrinsic CO_2 permeability of 720 Barrer (7,200 GPU permeance if 100 nm thick ZIF-8 membranes could be prepared). However, the ideal selectivity of ZIF-8 falls short of the commercial requirements with reported intrinsic CO_2/N_2 and CO_2/CH_4 ideal selectivities of 28 and 10, respectively [192]. Polycrystalline ZIF-8 membranes grown on α-Al_2O_3 discs [147,193], AAO discs [94,194], α-Al_2O_3 tubes [195], and polymer hollow fibers [97,130,139,142] for CO_2 separations have been reported. However, ideal selectivities of the prepared ZIF-8 membranes rarely exceed the value of 10. Other ZIF membranes including ZIF-7 [142], ZIF-69 [122], ZIF-90 [196], and ZIF-93 [88] have also been tested for CO_2 capture applications but none with standout performances. Polysulfone supported ultrathin (300 nm) ZIF-67 membranes prepared by Yu et al. [125] showed a promising CO_2/N_2 separation performances. The membrane displayed high CO_2 single gas permeance of 4257 GPU and CO_2/N_2 ideal selectivity of 56 owing to the existence of Co^{2+} open metal sites providing strong interaction with CO_2 molecules.

Mixed-linker route has recently gained popularity to tune the apertures of ZIFs to target CO_2/N_2 and CO_2/CH_4 mixtures. Hybrid ZIF-7-8 membrane is a particularly interesting one. A computational study by Krokidas et al. [197] demonstrated that incorporation of 33% of secondary benzimidazole (bIm) linkers in parent

ZIF-8 frameworks resulted in narrower apertures and higher CO_2/N_2 and CO_2/CH_4 diffusivity selectivities of 38 and 1900, respectively. Hillman et al. [43] observed a systematic shift towards a higher CO_2/CH_4 separation factor of their hybrid ZIF-7-8 membranes upon incorporation of up to 23% of bIm linkers in parent ZIF-8 frameworks. Despite having high bIm incorporation, CO_2/CH_4 separation factor did not improve by much possibly due to grain boundary effects and non-uniform distribution of secondary bIm linkers in the crystal grains. In another work, Eum et al. [147] performed 2-aminobenzimidazole (2abIm) ligand vapor phase treatment to tune the apertures of ZIF-8 towards smaller molecules. Incorporation of bulky 2abIm linkers in ZIF-8 framework improved molecular sieving effects. Ideal selectivities increased from 2.4 to 24 for CO_2/N_2 and from 2.2 to 32 for CO_2/CH_4 mixtures. On the other hand, CO_2 single gas permeances decreased to 195 GPU. ZIF-62 is an imidazole-benzimidazole (ImbIm) hybrid ZIF with a nominal composition of $Zn(Im)_{1.75}(bIm)_{0.25}$ [198]. Recently, Wang et al. [199] fabricated ~70 μm thick ZIF-62 glass membranes on α-Al_2O_3 discs by melt-quenching treatment. The MOF glass membranes showed high CO_2/N_2 and CO_2/CH_4 ideal selectivities of 35 and 37, respectively, owing to the absence of non-selective grain boundaries. Regrettably, the membrane displayed CO_2 single gas permeance of only 36 GPU possibly due to the thick membrane layer.

The underlying reasons behind poor performances of polycrystalline ZIF membranes for CO_2 capture applications is gate opening phenomenon and lattice flexibility. ZIFs with stiffer networks suppresses linker rotations and consequently improves ZIF molecular sieving capabilities [133]. Babu et al. [194] performed a novel rapid heat treatment (at 360 °C for a few seconds) to the as-prepared ZIF-8 membranes to distort and reduce flexibility of the frameworks. The heat-treated ZIF-8 membranes displayed attractive CO_2/N_2 and CO_2/CH_4 ideal selectivity as high as 29 and 23, respectively as illustrated in Fig. 11(a–c). Hou et al. [94] synthesized ZIF-7-8 membranes with suppressed linker mobility using current-driven synthesis. ZIF-7_{22}-8_{78} (22% incorporation of bIm linker in the frameworks) membranes exhibited better gas sieving due to more constricted pores (from bulky bIm linkers) and more rigid frameworks (from stiffer ZIF-8_Cm polymorph) as evidently shown in Fig. 11(d–f). The membranes showed CO_2 permeance of 45 GPU and CO_2/CH_4 separation factor of 25.

While there have been exciting findings reported, the research area of ZIFs for CO_2 capture applications is still at its infancy, requiring further developments. So far, we have seen pure and hybrid ZIF membranes with high CO_2 permselectivity or high CO_2 permeability, but not both. It is worth reminding the reader again that performances of these membranes are strongly dependent on the preparation method. Difficulties in preparing ZIF membranes with performances nearing its intrinsic transport properties send a clear message that preparing high quality polycrystalline ZIF membranes is a non-trivial task. To overcome these challenges, we believe the key here is to synthesize sub-100 nm thick membranes to improve throughput and utilize a combination of mixed-linker and framework stiffening approach to sharpen membrane molecular sieving properties. For instance, ~87 nm thick ZIF-8 membranes on PVDF hollow fibers prepared by Li et al. [130] exhibited CO_2 permeance as high as ~11,500 GPU, surpassing the commercial requirement of CO_2 permeance. As mentioned above, incorporating 33% of ZIF-7 linkers into ZIF-8 led to CO_2/N_2 and CO_2/CH_4 selectivity improvement to 38 and 1900, respectively [197]. By combining the aforementioned strategies, in combination with framework stiffening effect, we expect to obtain not only highly CO_2-productive but also CO_2-selective ZIF membranes.

Condensable gas separations

C_3 olefin/paraffin separations

Short-chain olefins, in particular ethylene (C_2H_4) and propylene (C_3H_6), are two of the largest chemical commodities used in the production of polymers and intermediates with a combined annual production of around 230 million tons [200]. Currently, olefin/paraffin separations are performed using thermally-driven distillation processes. With a difference in boiling points of only 4–5 °C, the distillation towers require a large number of distillation trays (100–150) and operate under a high reflux ratio (15–25), placing the olefin/paraffin separations among the highly capital and energy-intensive separation processes [10,201]. Industries are desperately looking for suitable alternatives for light hydrocarbon separations. Membrane technology has long been proposed as alternative to the conventional distillation process to produce high purity olefin. Unlike H_2 separation from N_2 or CO_2 removal from natural gas, separation of olefin from their respective paraffin are

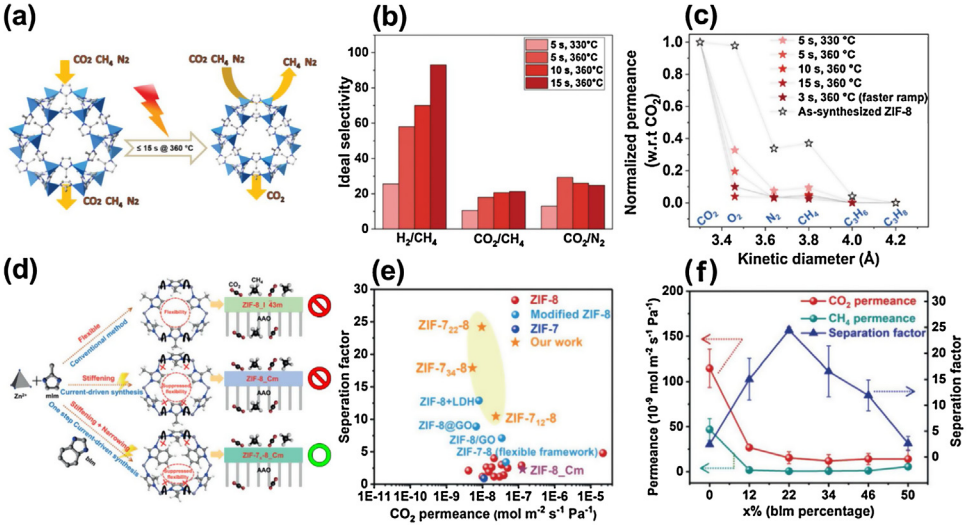

Fig. 11. (a) Schematic illustration of rapid heat treatment of ZIF-8. (b–c) Gas separation performances of ZIF-8 membranes as a function of dwell time. (d) Schematic illustration of the synthesis of hybrid ZIF-7-8 membranes. A combination of framework stiffening and pore narrowing improves CO_2/CH_4 selectivities. (e–f) CO_2/CH_4 separation performances of hybrid ZIF-7-8 membranes as a function of % incorporation of secondary bIm ligand in the frameworks. Adapted from Ref. [194] Copyright 2019 Wiley VCH and Ref. [94] Copyright 2018 John Wiley and Sons.

considered as one of the unsolved commercial application of membranes [10].

Among the different ZIF candidates, SOD ZIF-8 has received tremendous attention for C_3H_6/C_3H_8 separation due to its well-fitted effective apertures of 4.0–4.2 Å. Zhang et al. [39] back in 2012 demonstrated that framework flexibility was responsible for the enlargement of the six-membered rings of ZIF-8 beyond its XRD-derived apertures (3.4 Å). Based on the measured corrected diffusivities, the estimated C_3H_6/C_3H_8 diffusion selectivity of ZIF-8 was around 130. Membranes for commercial applications do not necessarily require high C_3H_6/C_3H_8 selectivity. Stable membranes with C_3H_6 permeance and C_3H_6/C_3H_8 selectivity of around 20–40 GPU and 6–10 are good enough to be used as membrane recovery unit in chemical reactor purge streams (e.g., polypropylene, isopropanol, and cumene) [18]. For larger targets such as replacing C_3 splitter column of hydrocarbon cracking unit, membranes with higher selectivity are needed. The most commonly mentioned reference of the required membrane performances to completely replace the C_3 splitter column is C_3H_6 permeance of 10 GPU (assuming the membrane can be fabricated around 0.1 μm thick) and C_3H_6/C_3H_8 separation factor of 35 [202].

One of the earliest reports of ZIF-8 membranes for C_3H_6/C_3H_8 separation was by Pan et al. [119] back in 2012. The average C_3H_6 permeance and C_3H_6/C_3H_8 separation factor of their ~2.0 μm thick ZIF-8 membranes were 83 GPU and 35, respectively. Among other early works on ZIF-8 membranes for C_3H_6/C_3H_8 separations were from Jeong's and Lin's groups [67,114,203]. Since then, we observe an explosive growth in ZIF-8 membrane research for C_3H_6/C_3H_8 separations and the researchers keep pushing C_3H_6/C_3H_8 separations limit of the membranes. Major activities in the area focus on the design of hybrid ZIFs crystals and membranes, development of better membrane processing, synthesis of ultrathin membranes, membrane synthesis on hollow fibers, and membrane microstructure control among other things, all to obtain better performing membranes in term of process economics. Consequently, numerous works of ZIF-8 membranes with state-of-the-art performances have been reported. The separation performances of ZIF-8, ZIF-67, and Co–Zn–ZIF-8 hybrid membranes for C_3H_6/C_3H_8 separations are summarized in Fig. 12. Majority of the recently published work reported membranes with performances far exceeding the commercial requirements proposed by Colling et al. [202].

ZIF membranes with ultrahigh C_3H_6 permeance and attractive C_3H_6/C_3H_8 separation factor are the result of superior membrane processing and precise molecular architecture of hybrid ZIFs. ZIF-8

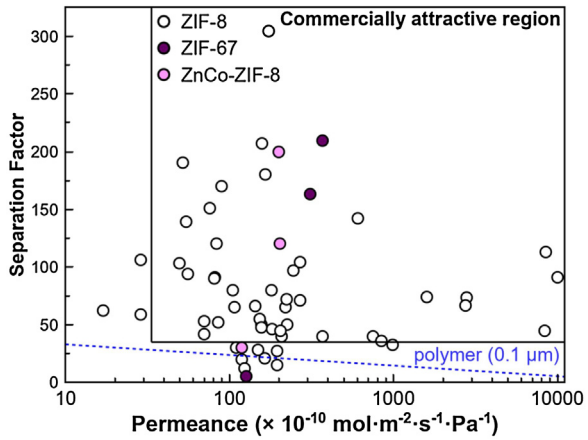

Fig. 12. C_3H_6/C_3H_8 separation performances of various ZIF membranes (i.e., ZIF-8 [44,67,71,76,77,79,84,95,101,105,114–117,119,120,127–130,132–135,140,148,203–224], Co–Zn–ZIF-8 [46,91,92], and ZIF-67 [107,220]) reported in literature (reported work from 2011 to 2021). The polymer upper bound were drawn based on Ref. [225].

membrane synthesized using the IMMP method by Eum's et al. [132], at 1 bar and 25 °C, displayed C_3H_6 permeance and C_3H_6/C_3H_8 separation factor of 45 GPU and 180, respectively. The membranes showed no significant deterioration in performances after continuous operation over 30 days. ZIF-8 membranes on yttria-stabilized zirconia hollow fibers and micromonolith prepared by Huang et al. [213] exhibited a high C_3H_6/C_3H_8 separation factor of 139. However, the membranes had a relatively low C_3H_6/C_3H_8 permeance of 16 GPU due to thick membranes. ZIF-8 membrane synthesized using microwave-assisted seeding and secondary growth method by Lee's et al. [209] showed C_3H_6 permeance of 47 GPU and C_3H_6/C_3H_8 separation factor of 207. In their follow up work, similar protocol was applied to synthesize sub-1 μm thick ZIF-8 membranes on Matrimid® 5218 hollow fibers showing C_3H_6 permeance and C_3H_6/C_3H_8 separation factor of 55 GPU and 46, respectively [117].

Synthesis of sub-500 nm thick ZIF membranes has become a focus of many research groups to maximize C_3H_6 throughput. 500 nm thick ZIF-8 membranes prepared by ENACT method showed high C_3H_6 permeance of 296 GPU. However, the reported C_3H_6/C_3H_8 separation factor was only 32, attributable to poor membrane grain boundary structures. Meanwhile, Wei et al. [128] fabricated 500 nm thick ZIF-8 membranes on AAO discs using cathodic deposition method. At room temperature and atmospheric pressure, the membrane displayed high C_3H_6 permeance and C_3H_6/C_3H_8 separation factor of 182 GPU and 142, respectively. Post-synthetic modification has also been used to synthesize ultrathin ZIF-8 membranes owing to labile nature of coordination bond of ZIFs. Lee et al. [95] drastically reduced the effective thickness of ZIF-8 membranes using post-synthetic linker exchange (PSLE). mIm linkers of ZIF-8 were partially exchanged with 2-imidazolecarboxaldehyde linkers (Ica, linker of ZIF-90) by immersing the ZIF-8 membranes into the Ica methanolic solution at 60 °C for several days. Incorporation of the daughter Ica linkers enlarged the ZIF-8 apertures, resulting in effective reduction in ZIF-8 membrane thickness. The hybrid ZIF-8-90 membranes displayed C_3H_6 permeance and C_3H_6/C_3H_8 separation factor of 232 GPU and 40, respectively. Considering the 4-fold increase in C_3H_6 permeance, the effective thickness of the ZIF-8 layer was estimated to have been reduced from 1 μm to 0.25 μm.

The unique nature of solvent-free vapor-phase synthesis enables the formation of even thinner ZIF membranes. The reported C_3H_6 permeances of the membranes prepared using this method is 10–50 times greater than majority of the reported values while still maintaining attractively high C_3H_6/C_3H_8 separation factor [79,130]. Ma et al. [79] reported vapor phase synthesis of ZIF-8 membranes with high C_3H_6 permeance of 480 GPU and C_3H_6/C_3H_8 separation factor of 74. ZIF-8 membranes prepared via gel-vapor transformation by Li et al. [130] displayed attractively high C_3H_6 permeance and C_3H_6/C_3H_8 separation factor of 824 GPU and 67, respectively, owing to their extremely thin selective layers of ~87 nm. Their even thinner ZIF-8 membranes (~17 nm) showed C_3H_6 permeance as high as 2500 GPU. Most recently, Qiao et al. [129] fabricated one of the thinnest ZIF-8 membranes on commercial polysulfone ultrafiltration substrates via interface layer polarization induction. 45 nm thick diethanolamine (DEA)-modified low crystallinity (LC) MOF membranes (DZIF-8) prepared using DEA concentration of 1.12×10^{-3} mol kg^{-1} currently hold the record of ZIF-8 membrane with highest C_3H_6 permeance of 3000 GPU while maintaining attractive C_3H_6/C_3H_8 separation factor of 90. The characteristic of the LC MOF membranes is they contain abundant of open metal sites, capable of forming π bond interactions with C_3H_6 molecules, thereby enhances transport of C_3H_6 molecules.

The intrinsic C_3H_6 permeability and C_3H_6/C_3H_8 diffusion selectivity of pure ZIF-8 crystals based on the kinetic uptake

(a)

Material or Membrane	C_3H_6 Permeability (Barrer)	C_3H_6/C_3H_8 Selectivity
MFI[a]	8085	2.24
ZIF-8[a]	390	135
ZIF-8 membrane: experimental[b]	371 ± 22	156 ± 26
ZIF-8/MFI MMM: experimental[b]	548 ± 67	146 ± 14
ZIF-8/MFI MMM: Maxwell model[c]	538	129

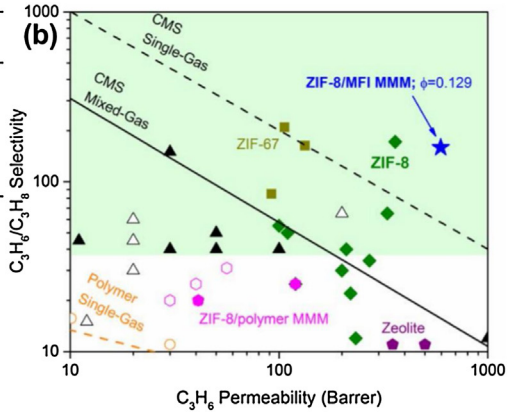

Fig. 13. (a) Permeabilities and selectivities of MFI and ZIF-8 obtained from adsorption and diffusion data.[a] Permeabilities and selectivities of ZIF-8 membranes and MFI/ZIF-8 MMMs measured using binary measurements at 1 bar.[b] Permeabilities and selectitivies of the all nanoporous hybrid MMMs calculated from the Maxwell model.[c] (b) Separation performances of MFI/ZIF-8 MMMs ($\varphi_{MFI} = 0.129 \pm 0.016$). Reproduced with permission from Ref. [136] Copyright 2019 Wiley VCH.

measurements are 390 Barrer and 130, respectively [39]. Theoretically speaking, C_3H_6/C_3H_8 separation performances of pure polycrystalline ZIF-8 membranes cannot exceed its intrinsic selectivity value. A concept of all nanoporous hybrid membrane is introduced to boost C_3H_6/C_3H_8 separation performances of ZIF-8 beyond its intrinsic transport properties. Though challenging, the upper-performance limit of ZIF-8 for C_3H_6/C_3H_8 be redefined by incorporating another nanoporous crystalline materials with permeability several order of magnitude higher than that of ZIF-8 [136]. The incorporation of more permeable nanoporous crystalline particles such as medium pore zeolites into ZIF-8 matrix allow access to a higher permeability and selectivity properties [204]. Using the previously explained IMMP, Rashidi et al. [136] reported MFI/ZIF-8 all nanoporous hybrid MMMs with higher C_3H_6 permeability (548 Barrer) and C_3H_6/C_3H_8 separation factor (146) (Fig. 13). The intrinsic C_3H_6 permeabilities and C_3H_6/C_3H_8 separation factor of the MFI/ZIF-8 hybrid materials ($\varphi_{MFI} = 0.129 \pm 0.016$) back-calculated using the Maxwell model were 538 Barrer and 129, respectively. The measured C_3H_6 permeability of the hybrid materials was 45% greater than the intrinsic permeability of ZIF-8. The upper-performance limit of ZIF-8 for C_3H_6/C_3H_8 separations can be further redefined with the introduction ZIF-8 membranes with distorted and stiffer frameworks via current-driven synthesis reported by Zhou et al. [133]. Enhanced C_3H_6/C_3H_8 molecular sieving effect of the newly discovered ZIF-8 polymorph (ZIF-8_Cm polymorph) resulted in ZIF-8 membranes with unprecedented separation factor of 304 (highest C_3H_6/C_3H_8 separation factor reported to date for ZIF membranes). The membranes also displayed good C_3H_6 permeance of 52 GPU.

Another candidate ZIF material for C_3H_6/C_3H_8 separation is Co-substituted ZIF-8 (i.e., ZIF-67). Narrower aperture fluctuation of ZIF-67 frameworks due to higher Co–N bond stiffness implies superior C_3H_6/C_3H_8 molecular sieving properties. Molecular dynamic simulation showed that ZIF-67 has C_3H_6/C_3H_8 corrected diffusivity ratio four times greater than that of ZIF-8, placing them to be among the top candidate materials for the challenging C_3H_6/C_3H_8 separations [40]. Kwon et al. [107] fabricated defect-free ZIF-67 membranes on α-Al_2O_3 discs by heteroepitaxially growing the ZIF-67 layer using ZIF-8 as seeds. The resulting membranes showed C_3H_6 permeance of 110 GPU and C_3H_6/C_3H_8 separation factor of 203, noticeably higher than separation performances of pure ZIF-8 membranes reported at that time. Since it is more difficult to prepare pure ZIF-67 membranes than that of ZIF-8, researchers substituted some of the Zn metals of ZIF-8 with Co to tune the effective pore apertures of the hybrid ZIFs [92].

Difficulty in preparing pure ZIF-67 membranes with optimized grain boundary structures is due to the fact that crystal nucleation and growth kinetics of ZIF-67 is faster than that of ZIF-8 [46]. Co_{50}–Zn_{50}–ZIF-8 membranes prepared by Hillman et al. [91] showed 100% improvement in C_3H_6/C_3H_8 separation factor as compared to the pure ZIF-8 membranes synthesized using similar method. The authors attributed the positive changes in C_3H_6/C_3H_8 separation factor to the increase in metal–nitrogen bond stiffness upon incorporation of Co into the frameworks which was confirmed by the blue-shift in IR metal-linker stretching frequency. Hou et al. [46] fabricated bimetallic ZIF-8 membranes (Co_{18}–Zn_{82}–ZIF-8) exhibiting impressively high C_3H_6 permeance and C_3H_6/C_3H_8 separation factor of 60 GPU and 200, respectively. Increasing Co content in the parent ZIF-8 frameworks did not necessarily result in better performing hybrid Co–Zn–ZIF-8 membranes due to competing effect between framework stiffness and grain boundary structures as illustrated in Fig. 14(b–c). Fig. 14(d) shows that the separation performances of the hybrid membranes were well-maintained even after 8 days of continuous operation indicating a long term stability.

Considering the effectiveness of ZIF (e.g., ZIF-8, ZIF-67, and Co–Zn–ZIF-8) membranes in isolating C_3H_6 from C_3H_8, it would be useful to perform process-scale assessments and economic evaluations of ZIF membrane system for commercial scale C_3H_6/C_3H_8 separations. There are a few notable works on techno-economic evaluations of membrane system for C_3H_6/C_3H_8 separations using process simulation package [21,79,226]. Amedi et al. [226] performed techno-economic feasibility studies of ZIF-8 membrane system which produce polymer grade propylene (99.8 mol%) using Aspen Hysys process simulator. Their simulation result showed that utilization of ZIF-8 membrane standalone unit with C_3H_6 permeance of 21 GPU and C_3H_6/C_3H_8 separation factor of 42 could save annual utility and operating cost by 67% and 46%, respectively. They also found that in a case where the membrane performance is much lower, running the membrane in a hybrid membrane-distillation mode is more economical compared to membrane only mode. In another work, Ma et al. [79] investigated the option of retrofitting ZIF-8 membrane unit into existing C_3 splitter column (i.e., hybrid mode) to produce 99.7 mol% purity C_3H_6 using Aspen Plus software. ZIF-8 membranes with rather conservative performances (i.e., C_3H_6 permeance of 100 GPU and selectivity of 50 at 7 bar) were selected for the simulation studies. At 7 bar pressure, the required membrane area to produce 250×10^3 tons polymer-grade C_3H_6 annually is $\sim$12,300 m^2 and a breakeven in capital cost can be achieved at membrane cost of

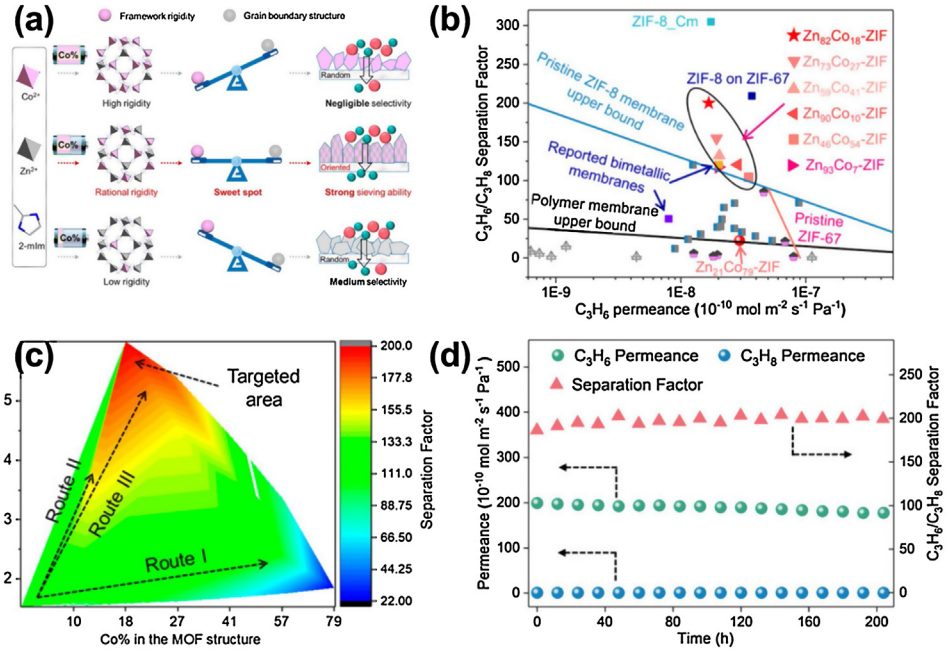

Fig. 14. (a) Schematic illustration of the design of hybrid Co–Zn–ZIF-8 membranes. A good balance between membrane grain boundary structure and lattice rigidity can result in membranes with optimum performances (b) Binary C_3H_6/C_3H_8 separation performances of Co–Zn–ZIF-8 membranes with various Co content in the ZIF-8 frameworks (c) A map showing the expected membrane performances of the hybrid Co–Zn–ZIF-8 membranes and several synthesis routes that can be used to achieve membranes with the desired performances (d) Time dependent permeation measurement of bimetallic Co–Zn–ZIF-8 membranes. Reproduced with permission from Ref. [46] Copyright 2020 American Chemical Society.

$130 per m^2. Meanwhile, a 25% capital cost saving can be achieved when operating the membrane system at pressure ratio of 15 bar. These results therefore indicate the economic potential of ZIF-8 membranes in industrial scale C_3H_6/C_3H_8 separations.

ZIF-8 membrane can also be utilized as membrane recovery unit or olefin recycling unit at purge stream of chemical reactor (e.g., polypropylene, iso-propanol, and cumene). From scale up point of view, application of ZIF-8 membrane as a recovery unit would be a more realistic short to medium term target as the C_3H_6 purity and membrane area requirements are much lower. For this particular application, C_3H_6 with purity of 80–90 mol% is adequate to be recycled back into the reactor [227]. Ma et al. [79] demonstrated that membrane with selectivity as low as 5 was able to recover 90% of C_3H_6 with purity >80 mol%. Note that the 90% of the recovered C_3H_6 is translated to roughly 11×10^3 tons of C_3H_6 per polypropylene plant per year that would otherwise lost/discarded in the purge stream [10]. Ability to recover C_3H_6 from the purge stream and recycle it back to the reactor result in a more productive chemical manufacturing process. A conservative estimate of the required membrane area to be deployed as membrane recovery unit in a typical size polypropylene plant using ZIF-8 membrane (C_3H_6 permeance of 100 GPU and C_3H_6/C_3H_8 separation factor of 5) is only ~250 m^2. From economic point of view, ZIF-8 membrane recovery unit with membrane cost of $500– $1000 per m^2 result in payback period of less than one year and 5-times return of investment during its first year of deployment [79]. The results therefore show that application of ZIF-8 membrane as olefin recycling unit not only economically viable but also able to generate high return on investment.

C_2 olefin/paraffin and C_4 isomers separations

Unlike C_3H_6/C_3H_8 separations, C_2H_4/C_2H_6 and n-C_4H_{10}/i-C_4H_{10} separations using ZIF membranes are not widely explored because there are no ZIFs with proper apertures and attractive transport properties. ZIF-8 effective pore apertures of 4.0 Å is ideal to isolate C_3H_6 from C_3H_8 but is too large for both C_2H_4 and C_2H_6 molecules. ZIF-8 single-crystal diffusivity measurements show high C_2H_4 and C_2H_6 diffusivities of 3.6×10^{-11} m^2 s^{-1} and 8.8×10^{-12} m^2 s^{-1}, respectively, but this result in unattractively low C_2H_4/C_2H_6 diffusivity selectivity of less than 3 [39,228–230]. Molecular simulation studies shows that ZIF-67 with stiffer metal-linker bonds can provide higher C_2H_4/C_2H_6 diffusivity ratio up to 9.4 compared to that of ZIF-8, but so far, there is no report on ZIF-67 membranes for C_2H_4/C_2H_6 separations [231]. Pure and hybrid ZIFs such as ZIF-4 [232], ZIF-7 [233], and the newly discovered GT-10 [234] have been utilized as adsorbent to separate C_2H_4 from C_2H_6 under kinetic or thermodynamic conditions but none have been prepared as C_2H_4-selective membranes.

For n-C_4H_{10}/i-C_4H_{10} separation, six-membered rings of ZIF-8 is too small to permit high diffusion of n-C_4H_{10} or i-C_4H_{10} into the cavities. ZIF-8 single-crystal measurements showed high n-C_4H_{10}/i-C_4H_{10} diffusion selectivity of around 2.5×10^6 but low n-C_4H_{10} diffusivity of only 5.7×10^{-16} m^2 s^{-1}. ZIF-90 having wider effective apertures of 5.0 Å able to effectively isolate n-C_4H_{10} from i-C_4H_{10} both with kinetic diameters of 4.7 Å and 5.3 Å, respectively [235]. Although the difference in the XRD-derived aperture between ZIF-90 and ZIF-8 is only 0.1 Å, ZIF-90 exhibits a sharp decline in gas permeabilities in n-C_4H_{10} and i-C_4H_{10} region. Single crystal diffusivity measurements show that ZIF-90 has n-C_4H_{10} diffusivity of 2.5×10^{-13} m^2·s^{-1} and n-C_4H_{10}/i-C_4H_{10} diffusivity selectivity of 700 [42]. Taking advantage of attractive transport properties of ZIF-90, Eum et al. [86] fabricated ~3.1 μm thick ZIF-90 membranes on macroporous carbon hollow fibers. At 25 °C and 1 bar, the membranes showed n-C_4H_{10} permeance of 60 GPU and n-C_4H_{10}/i-C_4H_{10} separation factor of 12. The n-C_4H_{10}/i-C_4H_{10} separation factor was lower than the reported single-crystal diffusivity data which can be attributed to poor membrane microstructures.

There have been attempts to tailor the n-C_4H_{10}/i-C_4H_{10} transport properties of ZIF-8 via post-synthetic thermal modification or hybrid ZIF approaches. Zhang and Koros [45] found that thermal dissociation of methyl groups (−CH_3) of mIm linkers at 400–500 °C enlarges the six-membered ring apertures of the ZIF-8.

After subjecting ZIF-8 crystals to a post-synthetic thermal modification, n-C_4H_{10} diffusivity of the thermally modified ZIF-8 increased by 28 times but still maintain relatively high n-C_4H_{10}/i-C_4H_{10} diffusion selectivity of 1.7×10^5 [45]. By incorporating a fraction of secondary Ica linkers in ZIF-8 frameworks, Eum et al. [42] managed to continuously tune the transport properties of n-C_4H_{10} and i-C_4H_{10} through the hybrid ZIF-8-90 crystals. To create a more open framework, our group incorporated unsubstituted imidazolate (Im) linkers into ZIF-8 frameworks using a delayed linker addition (DLA) method where the addition of secondary Im linkers in synthesis solution during microwave synthesis was purposely delayed [236]. Incorporation of 10 wt% of the Im_{52}-mIm_{48}-ZIF-8 powder into 6FDA-DAM polyimide resulted in MMMs with enhanced n-C_4H_{10} permeability of 18 Barrer and n-C_4H_{10}/i-C_4H_{10} ideal selectivity of 24. The reported permeability and selectivity of the Im_{52}-mIm_{48}-ZIF-8/6FDA-DAM MMMs were higher than the ZIF-8/6FDA-DAM MMMs, suggesting that the hybrid dual-linker ZIFs possess a more open frameworks. Despite showing promising performances, none of these hybrid ZIFs have been synthesized as supported polycrystalline membranes for n-C_4H_{10}/i-C_4H_{10} separations.

Future perspectives

Synthesis of polycrystalline membranes other than ZIF-8

From our review, we observed majority of works related to ZIF membrane focus on the synthesis of pure ZIF-8 membranes and their hybrid especially for C_3H_6/C_3H_8 separations. It is not surprising considering that ZIF-8 has robust synthesis as oppose to other ZIFs. As previously mentioned, the crystalline nature of ZIFs limits their aperture to a narrow size range which provides high molecular sieving for certain gas systems. That being said, the same material may not possess attractive gas transport properties for other gas mixtures. We believe future research should be directed to the synthesis of pure ZIF membranes other than ZIF-8. Among other ZIFs that are available, ZIF-7 and ZIF-90 materials deserve further investigation. ZIF-90 with SOD topology has an effective aperture of 5.0 Å making them attractive for n-C_4H_{10}/i-C_4H_{10} separations [42]. On the other hand, ZIF-7 with narrower apertures is better suited for H_2 separation from larger molecules such as CO_2, N_2, and CH_4 [37]. Both ZIFs, however, are not widely investigated compared to ZIF-8 as they are more difficult to synthesize.

Considering that it is significantly more challenging to synthesize high quality ZIF membranes other than ZIF-8, we propose to begin with high quality ZIF-8 membranes which can later be subjected to a post-synthetic modification (PSM) transforming the membranes into other ZIF membranes. Lee et al. [95] showed that mIm linkers of ZIF-8 can be exchanged with Ica linkers via liquid phase post-synthetic ligand exchange. Assuming that >90% ligand exchange process can be achieved without significant deterioration in membrane microstructures, the original high quality ZIF-8 membranes can be fully transformed into ZIF-90 membranes for n-C_4H_{10}/i-C_4H_{10} separation. Using a similar concept, a fraction ZIF-8 membrane can be transformed into ZIF-7 via liquid or vapor phase bIm linker exchange. Such membrane can be used for H_2 purifications. Wu et al. [237] managed to insert a series of secondary linkers such as 2-chloromethylbenzimidazole, 4-iodoimidazole, and 4-bromoimidazole into parent ZIF-8 frameworks using a vapor phase linker exchange (VPLT) tuning their gas adsorptive properties. In this case, PSM of MOFs/ZIFs (e.g., vapor-phase ligand exchange [237], solvent assisted ligand exchange [238], membrane surface ligand exchange [239], post-synthetic metal exchange [240], and post-synthetic thermal modification [45]) are indispensable to synthesize pure or hybrid ZIF membranes that are difficult to synthesize using conventional strategies. Besides, PSM can also be used to introduce certain functional groups or alter pore characters and surface environments of ZIFs which is not accessible from direct synthesis to obtain desired properties (e.g., enhanced stability, hydrophobicity and increase sorption capability) [241].

Hybrid SOD ZIF containing non-isostructural secondary linkers

For hybrid ZIFs, an interesting area worthwhile to be explored is in the synthesis of hybrid SOD ZIFs with secondary non-isostructural linkers and metals. There have been many reports on hybrid ZIF (e.g., ZIF-7-8 [43,94], ZIF-8-90 [42], 2abIm-ZIF-8 [147], Co–Zn–ZIF-8 [46], Cd–Zn–ZIF-8 [242], etc.) powders and membranes. However, the type of secondary metals and linkers used in the majority of the studies were isostructural, thereby enabling the hybrid ZIFs to maintain a similar topology. For example, mixing SOD ZIF-7 linkers (bIm) with SOD ZIF-8 linkers (mIm) result in a hybrid ZIF-7-8 where the SOD networks are maintained [43]. The choice of linkers and metals that can be incorporated to form isostructural hybrid ZIF are somewhat limited considering that there are not many SOD type ZIFs to begin with [93]. There have been several attempts to incorporate non-isostructural metals/linkers into SOD ZIFs. Schoenmakers [243] found that swapping Zn^{2+} of ZIF-8 with Cu^{2+} led to a formation of non-SOD ZIF-8. Cu^{2+} prefer octahedral coordination geometry as oppose to tetrahedral coordination geometry. Therefore, incorporation of Cu^{2+} disrupt the tetrahedral coordination of SOD ZIF-8 leading to formation of non-SOD ZIF structures. In other study, Huang et al. [244] mix two non-isostructural ZIF ligands (i.e., mIm linker of SOD ZIF-8 with 2-ethylimidazole ligand of ANA ZIF-14). As oppose to obtaining a single hybrid SOD ZIF-8-14 crystal, they ended up with a physical mixture of SOD ZIF-8 and a new phase with RHO topology. Hillman and Jeong [93] categorized ligands/metals that cannot form SOD ZIFs as ‘unsuitable’ and therefore cannot be incorporated in a high amount. Meanwhile, high percent linker/metal incorporation is required for the hybrid ZIFs to display noticeable changes in their transport properties.

Incorporation of non-isostructural ligands has been an interest of several groups to tune the aperture of ZIF-8. Replacing mIm ligands of ZIF-8 with imidazole (Im) ligands enlarges the apertures of the six-membered ring of the hybrid Im-mIm-ZIF-8. Such material can potentially be used to efficiently separate n-C_4H_{10} from i-C_4H_{10} [45]. For C_4 isomer separations, one might consider to just simply synthesize pure Im SOD ZIF-8 ($Zn(Im)_2$). However, Zn and Im rarely form porous frameworks as they are thermodynamically less stable but instead they form dense nets and nonporous polymorphs such as nog, cag, BCT, and zni [37,198,245,246]. This makes synthesis of SOD $Zn(Im)_2$ through direct hydro- or solvothermal approach challenging. In this case, incorporation of Im ligands into ZIF-8 frameworks can be an alternative to enlarge the apertures of the hybrid ZIFs. Development of a novel method to insert ‘unsuitable’ secondary metals and ligands into SOD ZIF frameworks in high amount can open up new possibilities for separation of other gas mixtures previously inaccessible with only pure ZIF or hybrid isostructural ZIF only.

In this case, molecular modeling and simulation software (e.g., Monte Carlo or molecular dynamics) are indispensable to screen for promising structures or design molecular architecture of hybrid SOD ZIFs to target specific applications [247]. Utilizations of molecular modeling enable researchers to determine the minimum fraction of secondary ligands or metals to be incorporated in parent ZIF frameworks as well as to predict the resulting sorption and diffusion selectivity of the hybrid ZIFs [40,197,231]. If the predicted transport properties of the new molecular sieve materials are attractive enough for the intended applications,

one can begin developing suitable synthesis protocols to prepare the proposed ZIF architectures.

ZIF-based mixed-matrix membranes

We cannot deny the fact that preparing polycrystalline ZIF membrane on porous substrates is challenging. Polycrystalline membranes by their very nature will always contain grain boundaries, with grain boundary channels larger than ZIF apertures. This has two implications. Firstly, the molecular sieving properties of polycrystalline ZIF membranes will always be inferior compared to single crystal ZIF membranes. The grain boundary channels, which are unavoidable features of ZIF membranes are considered as defects as they provide non-selective transport pathways for gas molecules through the membranes, hence undermining their overall performances [192]. Secondly, membranes separation properties are highly dependent on membranes processing. Slight changes in membrane processing result in different membrane microstructures, consequently, different membrane performances.

Because of these issues, researchers opt for a more straightforward mixed-matrix membranes (MMMs) approach. ZIF nanocrystals are a lot easier to be prepared than membranes. These fillers are then dispersed in a continuous polymer phase through a solution blending method. While the separation performances of ZIF-based MMMs are moderate compared to those of pure ZIFs, researchers gained advantages in term of membrane processability and reproducibility. For MMM fabrication, as long as the ZIF/polymer dope solution formulation is spinnable, the composite asymmetric hollow fiber membranes can be simply fabricated using the existing single- or dual-layer fiber spinning processes [5]. In fact, fabrication of ZIF/MOF-based hollow fiber MMMs using the conventional spinning technology have already been demonstrated [248,249]. In this section, we do not intend to provide a detailed discussion on recent progress in this area. There are many high quality reviews available in literature discussing different aspects of MMM synthesis (e.g., filler/polymer combinations, synthesis strategies, separation performances, interfacial defects, etc.) to keep the reader updated on the subject matter [57–61]. In this section, we would like to highlight several pioneering works that enable a scalable formation of asymmetric hollow fiber MMMs containing sub-1 μm thick selective skin layer for gas separations.

A conceptually feasible and economically attractive hollow fiber MMMs should possess (i) selective skin layer thickness between 200–500 nm (ii) accurate filler positioning in skin layer (iii) particle sizes < 20 nm (iv) porous sub-structure made from cheaper materials (v) ideal polymer/filler interface, all may not be able to be fulfilled using conventional solution blending method [5]. Difficulty in preparing high quality hollow fiber MMMs is due to the fact that formation of skin layer and filler incorporation occur concurrently. Knebel et al. [250] developed a readily dispersible ZIF in a solvent to form solution processible MMMs. Decorating outer surfaces of ZIF-67 with 1,3-bis(2,4,6-diisopropylphenyl)imidazole-2-ylidene (IDip) produced a stable dispersion of the particles in solvents such as cyclohexane which can later be processed into high loading MMMs. 47.5 wt% ZIF-67-IDip blended with 6FDA-DAM MMMs registered C_3H_6 permeability of 92 Barrer and C_3H_6/C_3H_8 separation factor of 14 which are 340% and 146% higher than that of neat 6FDA-DAM. Formulation of a stable dope solution is critical when fabricating hollow fiber MMMs as they affect stability of the fiber upon exiting the spinneret to form defect-free selective layer [5].

Our group came out with an innovative polymer-modification-metal-organic-framework-formation (PMMOF) technique with potential to suppress all engineering challenges mentioned above. In PMMOF, a preformed 6FDA-DAM polyimide coating on porous substrates undergone a series of steps (i.e., hydrolysis → ion-exchange → ligand treatment → reimidization) transforming the neat polymer into ZIF-8/6FDA-DAM MMMs while maintaining similar skin layer thickness. The PMMOFed membranes showed C_3H_6/C_3H_8 separation factor as high as 38, satisfying the commercial requirement despite using lower ZIF-8 loading (25.5 wt%), unattainable if using the conventional blending method. 60% incorporation of secondary ethylimidazole (eIm) linker in ZIF-8 fillers improved C_3H_6/C_3H_8 separation factor of the MMMs from 17 to 37. In this case, the filler loading in the MMMs was even lower around 12.3 wt% [48]. PMMOF method was also utilized to in-situ grow ZIF-7 nanofillers inside the polymer to form ZIF-7/6FDA-DAM MMMs for H_2 separations. In our follow up work, we demonstrated the first ever multi-strand hollow fiber ZIF-8/6FDA-DAM MMM modules showing promising C_3H_6/C_3H_8 separation performances. Seven polyethersulfone hollow fiber strands coated with thin (750 nm thick) 6FDA-DAM layers were in-situ transformed into ZIF-8 hollow fiber MMMs inside the modules. The membranes showed decent C_3H_6/C_3H_8 separation factor of 23 and C_3H_6 permeance of 2.14 GPU without additional defect plugging steps (>200% improvement in selectivity compared to pure 6FDA-DAM polyimide) [251]. The membrane performances were stable over the period of 25 days and at total feed pressure of 6 bar.

These findings are particularly important for a number of reason. In this new process, formation of neat polymer hollow fiber with optimized microstructures and MMM formation are decoupled. PMMOF is definitely a viable strategy and amenable to scale up. Massive engineering advantages can be achieved as one does not have to perform a major overhaul to existing hollow fiber spinning setup. Moreover, issues related to formulation of stable filler-containing dope solutions are eliminated altogether. In this process, we envisioned that formation of neat hollow fibers with thin skin layers of 6FDA-DAM can be done easily and reproducibly using existing fiber spinning setup. ZIF filler addition on the other hand can be performed inside a preformed module containing the neat hollow fibers, transforming polymer hollow fiber modules to MMM hollow fiber modules.

Realistic test condition and other technical challenges

One important aspect of ZIF membranes but often overlooked is membrane performances under high pressure conditions. In membrane operation, high pressure is required to provide sufficient driving force for gas transport through the membranes. Moreover, most feed gases to be processed are usually under high pressure. For instance, the pressure of C_3H_6/C_3H_8 mixtures output of hydrocarbon cracking unit and at isopropyl-alcohol reactor purge stream are around 20 bar [226,252]. There are only a handful of studies on high pressure measurements of ZIF membranes and the results are not encouraging. Hou et al. [46] observed the C_3H_6/C_3H_8 separation factor of Co_{18}–Zn_{82}–ZIF-8 membranes significantly decreased from 163 to 18 upon increasing feed gas pressure to 2.5 bar. Eum et al. [132] on the other hand reported a decline in C_3H_6/C_3H_8 separation factor by 50% as transmembrane pressure difference increased to 9 bar. Similarly, C_3H_6 permeance of the ZIF-8 membranes dropped by 51%. Decline in C_3H_6 permeance and C_3H_6/C_3H_8 separation factor at elevated pressure was attributed to combination of pressure-induced structural changes of flexible ZIF-8 frameworks and non-linear adsorption isotherm of C_3H_6 and C_3H_8 in ZIF-8 [55,253].

Coating ZIF membranes with caulking materials such as polydimethylsiloxane (PDMS) can help to prevent deterioration in membrane selectivity and permeance at elevated pressure. Sheng et al. [212] observed C_3H_6/C_3H_8 separation factor of the PDMS-coated ZIF-8 membranes increased by 12% upon increasing

transmembrane pressure difference to 6 bar. On the contrary, ZIF-8 membranes without PDMS coating registered 82% decrease in C_3H_6/C_3H_8 separation factor under a similar condition. Separation performances of the PDMS-coated ZIF-8 membranes under high pressure condition (6 bar) were well-maintained over a period of 2 months which indicate that the membranes have excellent long-term stability. In addition to stabilizing membrane performances under high pressure condition, PDMS also helps to repair membrane grain boundary defects, resulting in selectivity improvement [116]. Water stability of the PDMS-coated ZIF-8 also improves due to hydrophobic nature of the coating materials [212].

When it comes to scaling the technology up, another important aspect to consider is long term stability of the membrane. As previously mentioned, industrially relevant gas separation membranes should possess stable performances over a period of three to five years [18]. ZIF-8 membranes prepared by Eum et al. [132] maintained stable C_3H_6/C_3H_8 separation performances under continuous operation over a period of 1 month. Meanwhile, PDMS-coated ZIF-8 membrane by Sheng et al. [212] showed stable performance under high pressure condition of 6 bar for over 2 months of operations. Recently, Ma et al. [222] prepared ZIF-8 membranes on porous α-Al_2O_3 substrates via dip coating-thermal conversion (DCTC) method. Their ZIF-8 membranes exhibited stable C_3H_6/C_3H_8 separation performances over a span of 6 months. This remarkable stability of ZIF-8 membrane over long period hold great promise for commercialization.

In term of commercialization, more than 80% of the total installed gas separation modules are hollow fiber modules. The remaining 20% of the market is shared between spiral-wound and plate-and-frame modules, where the latter is a less popular choice among the two [11]. Given the brittle nature of ZIF membranes it is unlikely that the membrane to be packaged into spiral wound module leaving hollow fiber geometry as the most practical configuration. ZIF membranes should possess excellent mechanical properties to tolerate any mechanical stress that is introduced during membrane handling and module assembly process. To the best of our knowledge, there are only several papers studying mechanical property aspect of ZIF membranes. Mechanical testing (i.e., flexibility test) of the ZIF membrane involve simple bending test followed by gas separation measurements and microstructure evaluations. The membranes are assumed to have good mechanical properties if the membranes showed no formation of macroscopic cracks and maintained similar gas separation performances after subjected to bending test. H_2/CO_2 separation performances of ZIF-8 membranes on PVDF hollow fibers by Hou et al. [97] were well-maintained after bending with curvature of $\sim$77 m^{-1}. Note that curvature ($K = 1/r$) of a bending is a reciprocal of the bending radius (r). Integrity of the ZIF-8 membranes was not compromised after being subjected to 3% elongation (equivalent to tensile stress of 3.5 MPa). Zhao et al. [224] reported ZIF-8 membranes on polypropylene supports, showing high C_3H_6/C_3H_8 separation performances of 122 even after bending the flat membranes with a curvature of $\sim$92 m^{-1}. Polypropylene with a smaller Young's modulus than that of ZIF-8 was chosen as a substrate to provide greater flexibility, thereby reducing unwanted defect formation during bending test.

Despite the aforementioned advancements in ZIF membrane synthesis, the current approaches still retain several notable drawbacks: (i) large consumption of expensive precursors, (ii) use of toxic and non-eco-friendly organic solvents, (iii) slow batch processes, (iv) lengthy solvothermal or hydrothermal synthesis, and (v) use of expensive and specialized tools [74]. In term of cost, inorganic membranes (e.g., zeolite, MOF and ZIF) are prohibitively expensive, one- or two-order of magnitude higher than polymer membranes [62]. For ZIF membranes, we expect the overall membrane cost to be slightly lower than those of zeolites as membrane fabrication is less complex [254]. Significant effort should be dedicated for the development of cheaper and simpler membrane processing. Transitioning from planar to hollow fiber geometry, membrane modulation, and large area membrane synthesis are other important area that need to be looked into. In term of gas separation test, membrane researchers are also recommended to consider ternary/quaternary mixtures during permeation measurements and we might see interesting results along the way.

Final remarks

In the past few years, we have witnessed major developments in the synthesis of ultrathin ZIF and their hybrid membranes for separation applications. There are a wide variety of ZIF structures available to offer separation performances surpassing that of conventional polymers. Systematic adjustment of ZIF transport properties through hybrid approach and leveraging chemical functionalities of ZIF enable the materials to be utilized for other attractive applications. The scale up of supported ZIF membranes is among the challenge that need to be dealt with. Those grown on difficult-to-scale inorganic supports are expensive and current membrane manufacturing is unattractive as they involve complex non-continuous batch processes. As a final note, supported ZIF membranes still has a long way to go before it can be seriously considered for commercial applications. Academia, industries and government agencies need to work together to assess and tackle engineering challenges associated with membrane scale up to accelerate industrial adaptation of the technology.

Declaration of interest

No conflict of interest to declare.

Declaration of competing interest

The authors report no declarations of interest.

Acknowledgements

The authors acknowledge the financial supports by the Universiti Putra Malaysia under Geran Inisiatif Putra Muda (project code - GP-IPM/2020/9689700, vot no. - 9689700). H.-K.J. acknowledges the financial support from the National Science Foundation (CBET-1929596). This publication was made possible in part by NPRP grant # 12S-0209-190064 from the Qatar National Research Fund (a member of Qatar Foundation).

References

[1] D.S. Sholl, R.P. Lively, Nature 532 (2016) 435, doi:http://dx.doi.org/10.1038/532435a.
[2] J. Duan, Y. Pan, G. Liu, W. Jin, Curr. Opin. Chem. Eng. 20 (2018) 122, doi:http://dx.doi.org/10.1016/j.coche.2018.04.005.
[3] J. Caro, Curr. Opin. Chem. Eng. 1 (2011) 77, doi:http://dx.doi.org/10.1016/j.coche.2011.08.007.
[4] E. Adatoz, A.K. Avci, S. Keskin, Sep. Purif. Technol. 152 (2015) 207, doi:http://dx.doi.org/10.1016/j.seppur.2015.08.020.
[5] M.R. Abdul Hamid, H.-K. Jeong, Korean J. Chem. Eng. 35 (2018) 1577, doi:http://dx.doi.org/10.1007/s11814-018-0081-1.
[6] Q. Qian, P.A. Asinger, M.J. Lee, G. Han, K. Mizrahi Rodriguez, S. Lin, F.M. Benedetti, A.X. Wu, W.S. Chi, Z.P. Smith, Chem. Rev. 120 (2020) 8161, doi:http://dx.doi.org/10.1021/acs.chemrev.0c00119.
[7] Z. Kang, L. Fan, D. Sun, J. Mater. Chem. A 5 (2017) 10073, doi:http://dx.doi.org/10.1039/C7TA01142C.
[8] C. Zhang, B.-H. Wu, M.-Q. Ma, Z. Wang, Z.-K. Xu, Chem. Soc. Rev. 48 (2019) 3811, doi:http://dx.doi.org/10.1039/C9CS00322C.
[9] S. Qiu, M. Xue, G. Zhu, Chem. Soc. Rev. 43 (2014) 6116, doi:http://dx.doi.org/10.1039/C4CS00159A.
[10] M. Galizia, W.S. Chi, Z.P. Smith, T.C. Merkel, R.W. Baker, B.D. Freeman, Macromolecules 50 (2017) 7809, doi:http://dx.doi.org/10.1021/acs.macromol.7b01718.

[11] R.W. Baker, Ind. Eng. Chem. Res. 41 (2002) 1393, doi:http://dx.doi.org/10.1021/ie0108088.
[12] P. Bernardo, E. Drioli, G. Golemme, Ind. Eng. Chem. Res. 48 (2009) 4638, doi:http://dx.doi.org/10.1021/ie8019032.
[13] L.M. Robeson, J. Membr. Sci. 320 (2008) 390, doi:http://dx.doi.org/10.1016/j.memsci.2008.04.030.
[14] Y. Ding, Ind. Eng. Chem. Res. 59 (2019) 556, doi:http://dx.doi.org/10.1021/acs.iecr.9b05975.
[15] G.M. Iyer, L. Liu, C. Zhang, J. Polym. Sci. 58 (2020) 2482, doi:http://dx.doi.org/10.1002/pol.20200128.
[16] Y. Xiao, B.T. Low, S.S. Hosseini, T.S. Chung, D.R. Paul, Prog. Polym. Sci. 34 (2009) 561, doi:http://dx.doi.org/10.1016/j.progpolymsci.2008.12.004.
[17] M.S. Suleman, K.K. Lau, Y.F. Yeong, Chem. Eng. Technol. 39 (2016) 1604, doi:http://dx.doi.org/10.1002/ceat.201500495.
[18] R.W. Baker, B.T. Low, Macromolecules 47 (2014) 6999, doi:http://dx.doi.org/10.1021/ma501488s.
[19] Y. Ren, X. Liang, H. Dou, C. Ye, Z. Guo, J. Wang, Y. Pan, H. Wu, M.D. Guiver, Z. Jiang, Adv. Sci. 7 (2020)2001398, doi:http://dx.doi.org/10.1002/advs.202001398.
[20] L. Li, R.-B. Lin, R. Krishna, H. Li, S. Xiang, H. Wu, J. Li, W. Zhou, B. Chen, Science 362 (2018) 443, doi:http://dx.doi.org/10.1126/science.aat0586.
[21] U. Lee, J. Kim, I. Seok Chae, C. Han, Chem. Eng. Process 119 (2017) 62, doi:http://dx.doi.org/10.1016/j.cep.2017.05.013.
[22] N. Kosinov, J. Gascon, F. Kapteijn, E.J.M. Hensen, J. Membr. Sci. 499 (2016) 65, doi:http://dx.doi.org/10.1016/j.memsci.2015.10.049.
[23] J.B.S. Hamm, A. Ambrosi, J.G. Griebeler, N.R. Marcilio, I.C. Tessaro, L.D. Pollo, Int. J. Hydrogen Energy 42 (2017) 24830, doi:http://dx.doi.org/10.1016/j.ijhydene.2017.08.071.
[24] B.M. Yoo, J.E. Shin, H.D. Lee, H.B. Park, Curr. Opin. Chem. Eng. 16 (2017) 39, doi:http://dx.doi.org/10.1016/j.coche.2017.04.004.
[25] S. Liguori, K. Kian, N. Buggy, B.H. Anzelmo, J. Wilcox, Prog. Energy Combust. Sci. 80 (2020)100851, doi:http://dx.doi.org/10.1016/j.pecs.2020.100851.
[26] O.K. Farha, J.T. Hupp, Acc. Chem. Res. 43 (2010) 1166, doi:http://dx.doi.org/10.1021/ar1000617.
[27] J.-R. Li, J. Sculley, H.-C. Zhou, Chem. Rev. 112 (2012) 869, doi:http://dx.doi.org/10.1021/cr200190s.
[28] G. Férey, Chem. Soc. Rev. 37 (2008) 191, doi:http://dx.doi.org/10.1039/B618320B.
[29] H. Furukawa, K.E. Cordova, M. O'Keeffe, O.M. Yaghi, Science 341 (2013), doi:http://dx.doi.org/10.1126/science.1230444.
[30] H.-C. Zhou, J.R. Long, O.M. Yaghi, Chem. Rev. 112 (2012) 673, doi:http://dx.doi.org/10.1021/cr300014x.
[31] H. Li, K. Wang, Y. Sun, C.T. Lollar, J. Li, H.-C. Zhou, Mater. Today 21 (2018) 108, doi:http://dx.doi.org/10.1016/j.mattod.2017.07.006.
[32] R.-B. Lin, S. Xiang, H. Xing, W. Zhou, B. Chen, Coord. Chem. Rev. 378 (2019) 87, doi:http://dx.doi.org/10.1016/j.ccr.2017.09.027.
[33] J. Lee, O.K. Farha, J. Roberts, K.A. Scheidt, S.T. Nguyen, J.T. Hupp, Chem. Soc. Rev. 38 (2009) 1450, doi:http://dx.doi.org/10.1039/B807080F.
[34] P. Kumar, A. Deep, K.-H. Kim, Trends Anal. Chem. 73 (2015) 39, doi:http://dx.doi.org/10.1016/j.trac.2015.04.009.
[35] Y. Sun, L. Zheng, Y. Yang, X. Qian, T. Fu, X. Li, Z. Yang, H. Yan, C. Cui, W. Tan, Nanomicro Lett. 12 (2020) 1, doi:http://dx.doi.org/10.1007/s40820-020-00423-3.
[36] B. Wang, A.P. Côté, H. Furukawa, M. O'Keeffe, O.M. Yaghi, Nature 453 (2008) 207, doi:http://dx.doi.org/10.1038/nature06900.
[37] K.S. Park, Z. Ni, A.P. Côté, J.Y. Choi, R. Huang, F.J. Uribe-Romo, H.K. Chae, M. O'Keeffe, O.M. Yaghi, Proc. Natl. Acad. Sci. U. S. A. 103 (2006) 10186, doi:http://dx.doi.org/10.1073/pnas.0602439103.
[38] A. Phan, C.J. Doonan, F.J. Uribe-Romo, C.B. Knobler, M. O'Keeffe, O.M. Yaghi, Acc. Chem. Res. 43 (2010) 58, doi:http://dx.doi.org/10.1021/ar900116g.
[39] C. Zhang, R.P. Lively, K. Zhang, J.R. Johnson, O. Karvan, W.J. Koros, J. Phys. Chem. Lett. 3 (2012) 2130, doi:http://dx.doi.org/10.1021/jz300855a.
[40] P. Krokidas, M. Castier, S. Moncho, D.N. Sredojevic, E.N. Brothers, H.T. Kwon, H.-K. Jeong, J.S. Lee, I.G. Economou, J. Phys. Chem. C 120 (2016) 8116, doi:http://dx.doi.org/10.1021/acs.jpcc.6b00305.
[41] W. Morris, C.J. Doonan, H. Furukawa, R. Banerjee, O.M. Yaghi, J. Am. Chem. Soc. 130 (2008) 12626, doi:http://dx.doi.org/10.1021/ja805222x.
[42] K. Eum, K.C. Jayachandrababu, F. Rashidi, K. Zhang, J. Leisen, S. Graham, R.P. Lively, R.R. Chance, D.S. Sholl, C.W. Jones, J. Am. Chem. Soc. 137 (2015) 4191, doi:http://dx.doi.org/10.1021/jacs.5b00803.
[43] F. Hillman, J. Brito, H.-K. Jeong, ACS Appl. Mater. Interfaces 10 (2018) 5586, doi:http://dx.doi.org/10.1021/acsami.7b18506.
[44] J.B. James, L. Lang, L. Meng, J.Y.S. Lin, ACS Appl. Mater. Interfaces 12 (2019) 3893, doi:http://dx.doi.org/10.1021/acsami.9b19964.
[45] C. Zhang, W.J. Koros, ACS Appl. Mater. Interfaces 7 (2015) 23407, doi:http://dx.doi.org/10.1021/acsami.5b07769.
[46] Q. Hou, S. Zhou, Y. Wei, J. Caro, H. Wang, J. Am. Chem. Soc. 142 (2020) 9582, doi:http://dx.doi.org/10.1021/jacs.0c02181.
[47] J.A. Thompson, J.T. Vaughn, N.A. Brunelli, W.J. Koros, C.W. Jones, S. Nair, Microporous Mesoporous Mater. 192 (2014) 43, doi:http://dx.doi.org/10.1016/j.micromeso.2013.06.036.
[48] S. Park, H.-K. Jeong, J. Membr. Sci. 596 (2020)117689, doi:http://dx.doi.org/10.1016/j.memsci.2019.117689.
[49] J. Hou, H. Zhang, G.P. Simon, H. Wang, Adv. Mater. 32 (2020)1902009, doi:http://dx.doi.org/10.1002/adma.201902009.
[50] D.J. Babu, G. He, L.F. Villalobos, K.V. Agrawal, ACS Sustain. Chem. Eng. 7 (2018) 49, doi:http://dx.doi.org/10.1021/acssuschemeng.8b05409.
[51] B. Chen, Z. Yang, Y. Zhu, Y. Xia, J. Mater. Chem. A 2 (2014) 16811, doi:http://dx.doi.org/10.1039/C4TA02984D.
[52] V.M.A. Melgar, J. Kim, M.R. Othman, J. Ind. Eng. Chem. 28 (2015) 1, doi:http://dx.doi.org/10.1016/j.jiec.2015.03.006.
[53] X. Ma, D. Liu, Crystals 9 (2019) 14, doi:http://dx.doi.org/10.3390/cryst9010014.
[54] L. Yang, S. Qian, X. Wang, X. Cui, B. Chen, H. Xing, Chem. Soc. Rev. 49 (2020) 5359, doi:http://dx.doi.org/10.1039/C9CS00756C.
[55] C. Zhang, Y. Dai, J.R. Johnson, O. Karvan, W.J. Koros, J. Membr. Sci. 389 (2012) 34, doi:http://dx.doi.org/10.1016/j.memsci.2011.10.003.
[56] S. Park, M.R. Abdul Hamid, H.-K. Jeong, ACS Appl. Mater. Interfaces 11 (2019) 25949, doi:http://dx.doi.org/10.1021/acsami.9b07106.
[57] W. Guan, Y. Dai, C. Dong, X. Yang, Y. Xi, J. Appl. Polym. Sci. 137 (2020) 48968, doi:http://dx.doi.org/10.1002/app.48968.
[58] M. Vinoba, M. Bhagiyalakshmi, Y. Alqaheem, A.A. Alomair, A. Pérez, M.S. Rana, Sep. Purif. Technol. 188 (2017) 431, doi:http://dx.doi.org/10.1016/j.seppur.2017.07.051.
[59] Y. Shi, B. Liang, R.-B. Lin, C. Zhang, B. Chen, Trends Chem. 2 (2020) 254, doi:http://dx.doi.org/10.1016/j.trechm.2020.01.002.
[60] Y. Cheng, Z. Wang, D. Zhao, Ind. Eng. Chem. Res. 57 (2018) 4139, doi:http://dx.doi.org/10.1021/acs.iecr.7b04796.
[61] M. Wang, Z. Wang, S. Zhao, J. Wang, S. Wang, Chin. J. Chem. Eng. 25 (2017) 1581, doi:http://dx.doi.org/10.1016/j.cjche.2017.07.006.
[62] Y.S. Lin, Ind. Eng. Chem. Res. 58 (2018) 5787, doi:http://dx.doi.org/10.1021/acs.iecr.8b04539.
[63] S. Smart, C.X.C. Lin, L. Ding, K. Thambimuthu, J.C.D. Da Costa, Energy Environ. Sci. 3 (2010) 268, doi:http://dx.doi.org/10.1039/B924327E.
[64] J. Caro, Chem. Soc. Rev. 45 (2016) 3468, doi:http://dx.doi.org/10.1039/C5CS00597C.
[65] J. Caro, M. Noack, P. Kölsch, R. Schäfer, Microporous Mesoporous Mater. 38 (2000) 3, doi:http://dx.doi.org/10.1016/S1387-1811(99)00295-4.
[66] M.C. Lovallo, A. Gouzinis, M. Tsapatsis, AIChE J. 44 (1998) 1903, doi:http://dx.doi.org/10.1002/aic.690440820.
[67] H.T. Kwon, H.-K. Jeong, J. Am. Chem. Soc. 135 (2013) 10763, doi:http://dx.doi.org/10.1021/ja403849c.
[68] P. Yang, Z. Li, Z. Gao, M. Song, J. Zhou, Q. Fang, M. Xue, S. Qiu, ACS Sustain. Chem. Eng. 7 (2019) 4158, doi:http://dx.doi.org/10.1021/acssuschemeng.8b05764.
[69] K. Kida, K. Fujita, T. Shimada, S. Tanaka, Y. Miyake, Dalton Trans. 42 (2013) 11128, doi:http://dx.doi.org/10.1039/C3DT51135A.
[70] J. Yao, D. Dong, D. Li, L. He, G. Xu, H. Wang, ChemComm 47 (2011) 2559, doi:http://dx.doi.org/10.1039/C0CC04734A.
[71] E. Barankova, X. Tan, L.F. Villalobos, E. Litwiller, K.V. Peinemann, Angew. Chem. Int. Ed. 56 (2017) 2965, doi:http://dx.doi.org/10.1002/anie.201611927.
[72] H. Bux, F. Liang, Y. Li, J. Cravillon, M. Wiebcke, J.r. Caro, J. Am. Chem. Soc. 131 (2009) 16000, doi:http://dx.doi.org/10.1021/ja907359t.
[73] V.M.A. Melgar, H. Ahn, J. Kim, M.R. Othman, J. Ind. Eng. Chem. 21 (2015) 575, doi:http://dx.doi.org/10.1016/j.jiec.2014.03.021.
[74] V.M.A. Melgar, H.T. Kwon, J. Kim, J. Membr. Sci. 459 (2014) 190, doi:http://dx.doi.org/10.1016/j.memsci.2014.02.020.
[75] B.P. Biswal, A. Bhaskar, R. Banerjee, U.K. Kharul, Nanoscale 7 (2015) 7291, doi:http://dx.doi.org/10.1039/C5NR00299K.
[76] A.J. Brown, N.A. Brunelli, K. Eum, F. Rashidi, J.R. Johnson, W.J. Koros, C.W. Jones, S. Nair, Science 345 (2014) 72, doi:http://dx.doi.org/10.1126/science.1251181.
[77] J. Yu, Y. Pan, C. Wang, Z. Lai, Chem. Eng. Sci. 141 (2016) 119, doi:http://dx.doi.org/10.1016/j.ces.2015.10.035.
[78] M. Drobek, M. Bechelany, C. Vallicari, A. Abou Chaaya, C. Charmette, C. Salvador-Levehang, P. Miele, A. Julbe, J. Membr. Sci. 475 (2015) 39, doi:http://dx.doi.org/10.1016/j.memsci.2014.10.011.
[79] X. Ma, P. Kumar, N. Mittal, A. Khlyustova, P. Daoutidis, K.A. Mkhoyan, M. Tsapatsis, Science 361 (2018) 1008, doi:http://dx.doi.org/10.1126/science.aat4123.
[80] Y. Go, J.H. Lee, I.K. Shamsudin, J. Kim, M.R. Othman, Int. J. Hydrogen Energy 41 (2016) 10366, doi:http://dx.doi.org/10.1016/j.ijhydene.2015.09.060.
[81] Y. Wang, H. Zhang, X. Wang, C. Zou, B. Meng, X. Tan, Ind. Eng. Chem. Res. 58 (2019) 19511, doi:http://dx.doi.org/10.1021/acs.iecr.9b04464.
[82] J. Liu, C. Liu, A. Huang, Int. J. Hydrogen Energy 45 (2020) 703, doi:http://dx.doi.org/10.1016/j.ijhydene.2019.10.230.
[83] A. Huang, H. Bux, F. Steinbach, J. Caro, Angew. Chem. 122 (2010) 5078, doi:http://dx.doi.org/10.1002/ange.201001919.
[84] N.T. Tran, H.T. Kwon, W.-S. Kim, J. Kim, Mater. Lett. 271 (2020)127777, doi:http://dx.doi.org/10.1016/j.matlet.2020.127777.
[85] X. Dong, K. Huang, S. Liu, R. Ren, W. Jin, Y.S. Lin, J. Mater. Chem. 22 (2012) 19222, doi:http://dx.doi.org/10.1039/C2JM34102F.
[86] K. Eum, C. Ma, D.Y. Koh, F. Rashidi, Z. Li, C.W. Jones, R.P. Lively, S. Nair, Adv. Mater. Interfaces 4 (2017)1700080, doi:http://dx.doi.org/10.1002/admi.201700080.
[87] A. Huang, Q. Liu, N. Wang, J. Caro, Microporous Mesoporous Mater. 192 (2014) 18, doi:http://dx.doi.org/10.1016/j.micromeso.2013.09.025.
[88] F. Cacho-Bailo, G. Caro, M. Etxeberría-Benavides, O. Karvan, C. Téllez, J. Coronas, ChemComm 51 (2015) 11283, doi:http://dx.doi.org/10.1039/C5CC03937A.

[89] A. Huang, Y. Chen, N. Wang, Z. Hu, J. Jiang, J. Caro, ChemComm 48 (2012) 10981, doi:http://dx.doi.org/10.1039/C2CC35691K.
[90] N. Wang, Y. Liu, Z. Qiao, L. Diestel, J. Zhou, A. Huang, J. Caro, J. Mater. Chem. A 3 (2015) 4722, doi:http://dx.doi.org/10.1039/C4TA06763K.
[91] F. Hillman, J.M. Zimmerman, S.-M. Paek, M.R. Abdul Hamid, W.T. Lim, H.-K. Jeong, J. Mater. Chem. A 5 (2017) 6090, doi:http://dx.doi.org/10.1039/C6TA11170J.
[92] C. Wang, F. Yang, L. Sheng, J. Yu, K. Yao, L. Zhang, Y. Pan, ChemComm 52 (2016) 12578, doi:http://dx.doi.org/10.1039/C6CC06457D.
[93] F. Hillman, H.-K. Jeong, ACS Appl. Mater. Interfaces 11 (2019) 18377, doi:http://dx.doi.org/10.1021/acsami.9b02114.
[94] Q. Hou, Y. Wu, S. Zhou, Y. Wei, J. Caro, H. Wang, Angew. Chem. Int. Ed. 58 (2019) 327, doi:http://dx.doi.org/10.1002/anie.201811638.
[95] M.J. Lee, H.T. Kwon, H.K. Jeong, Angew. Chem. Int. Ed. 57 (2018) 156, doi:http://dx.doi.org/10.1002/anie.201708924.
[96] A. Huang, Q. Liu, N. Wang, J. Caro, J. Mater. Chem. A 2 (2014) 8246, doi:http://dx.doi.org/10.1039/C4TA00299G.
[97] J. Hou, P.D. Sutrisna, Y. Zhang, V. Chen, Angew. Chem. Int. Ed. 55 (2016) 3947, doi:http://dx.doi.org/10.1002/anie.201511340.
[98] W. Li, Q. Meng, C. Zhang, G. Zhang, Chem. Eur. J. 21 (2015) 7224, doi:http://dx.doi.org/10.1002/chem.201500007.
[99] Q. Liu, N. Wang, J.r. Caro, A. Huang, J. Am. Chem. Soc. 135 (2013) 17679, doi:http://dx.doi.org/10.1021/ja4080562.
[100] K. Huang, Z. Dong, Q. Li, W. Jin, ChemComm 49 (2013) 10326, doi:http://dx.doi.org/10.1039/C3CC46244G.
[101] X. Jiang, S. Li, Y. Bai, L. Shao, J. Mater. Chem. A 7 (2019) 10898, doi:http://dx.doi.org/10.1039/C8TA11748A.
[102] X. Ruan, X. Zhang, Z. Zhou, X. Jiang, Y. Dai, X. Yan, G. He, Sep. Purif. Technol. 214 (2019) 95, doi:http://dx.doi.org/10.1016/j.seppur.2018.02.049.
[103] S. Tanaka, T. Shimada, K. Fujita, Y. Miyake, K. Kida, K. Yogo, J.F.M. Denayer, M. Sugita, T. Takewaki, J. Membr. Sci. 472 (2014) 29, doi:http://dx.doi.org/10.1016/j.memsci.2014.08.038.
[104] A. Huang, W. Dou, J.r. Caro, J. Am. Chem. Soc. 132 (2010) 15562, doi:http://dx.doi.org/10.1021/ja108774v.
[105] H.T. Kwon, H.-K. Jeong, Chem. Eng. Sci. 124 (2015) 20, doi:http://dx.doi.org/10.1016/j.ces.2014.06.021.
[106] M.C. McCarthy, V. Varela-Guerrero, G.V. Barnett, H.-K. Jeong, Langmuir 26 (2010) 14636, doi:http://dx.doi.org/10.1021/la102409e.
[107] H.T. Kwon, H.-K. Jeong, A.S. Lee, H.S. An, J.S. Lee, J. Am. Chem. Soc. 137 (2015) 12304, doi:http://dx.doi.org/10.1021/jacs.5b06730.
[108] Z. Lai, G. Bonilla, I. Diaz, J.G. Nery, K. Sujaoti, M.A. Amat, E. Kokkoli, O. Terasaki, R.W. Thompson, M. Tsapatsis, Science 300 (2003) 456, doi:http://dx.doi.org/10.1126/science.1082169.
[109] Z. Lai, M. Tsapatsis, J.P. Nicolich, Adv. Funct. Mater. 14 (2004) 716, doi:http://dx.doi.org/10.1002/adfm.200400040.
[110] Y. Liu, Y. Li, W. Yang, J. Am. Chem. Soc. 132 (2010) 1768, doi:http://dx.doi.org/10.1021/ja909888v.
[111] K. Tao, C. Kong, L. Chen, Chem. Eng. J. 220 (2013) 1, doi:http://dx.doi.org/10.1016/j.cej.2013.01.051.
[112] H. Chang, Y. Wang, L. Xiang, D. Liu, C. Wang, Y. Pan, Chem. Eng. Sci. 192 (2018) 85, doi:http://dx.doi.org/10.1016/j.ces.2018.07.027.
[113] X. Zhang, Y. Liu, L. Kong, H. Liu, J. Qiu, W. Han, L.-T. Weng, K.L. Yeung, W. Zhu, J. Mater. Chem. A 1 (2013) 10635, doi:http://dx.doi.org/10.1039/C3TA12234D.
[114] H.T. Kwon, H.-K. Jeong, ChemComm 49 (2013) 3854, doi:http://dx.doi.org/10.1039/C3CC41039K.
[115] M.R. Abdul Hamid, S. Park, J.S. Kim, Y.M. Lee, H.-K. Jeong, Ind. Eng. Chem. Res. 58 (2019) 14947, doi:http://dx.doi.org/10.1021/acs.iecr.9b02969.
[116] M.R. Abdul Hamid, H.-K. Jeong, J. Ind. Eng. Chem. 88 (2020) 319, doi:http://dx.doi.org/10.1016/j.jiec.2020.04.031.
[117] M.J. Lee, M.R. Abdul Hamid, J. Lee, J.S. Kim, Y.M. Lee, H.-K. Jeong, J. Membr. Sci. 559 (2018) 28, doi:http://dx.doi.org/10.1016/j.memsci.2018.04.041.
[118] Y. Li, F. Liang, H. Bux, W. Yang, J. Caro, J. Membr. Sci. 354 (2010) 48, doi:http://dx.doi.org/10.1016/j.memsci.2010.02.074.
[119] Y. Pan, T. Li, G. Lestari, Z. Lai, J. Membr. Sci. 390 (2012) 93, doi:http://dx.doi.org/10.1016/j.memsci.2011.11.024.
[120] Y. Pan, Z. Lai, ChemComm 47 (2011) 10275, doi:http://dx.doi.org/10.1039/C1CC14051E.
[121] H. Bux, A. Feldhoff, J. Cravillon, M. Wiebcke, Y.-S. Li, J. Caro, Chem. Mater. 23 (2011) 2262, doi:http://dx.doi.org/10.1021/cm200555s.
[122] Y. Liu, G. Zeng, Y. Pan, Z. Lai, J. Membr. Sci. 379 (2011) 46, doi:http://dx.doi.org/10.1016/j.memsci.2011.05.041.
[123] N. Rangnekar, N. Mittal, B. Elyassi, J. Caro, M. Tsapatsis, Chem. Soc. Rev. 44 (2015) 7128, doi:http://dx.doi.org/10.1039/C5CS00292C.
[124] M. Tsapatsis, Science 334 (2011) 767, doi:http://dx.doi.org/10.1126/science.1205957.
[125] C. Yu, Y. Liang, W. Xue, Z. Zhang, X. Jia, H. Huang, Z. Qiao, D. Mei, C. Zhong, J. Membr. Sci. 625 (2021)119139, doi:http://dx.doi.org/10.1016/j.memsci.2021.119139.
[126] H.T. Kwon, H.-K. Jeong, A.S. Lee, H.S. An, T. Lee, E. Jang, J.S. Lee, J. Choi, ChemComm 52 (2016) 11669, doi:http://dx.doi.org/10.1039/C6CC05433A.
[127] G. He, M. Dakhchoune, J. Zhao, S. Huang, K.V. Agrawal, Adv. Funct. Mater. 28 (2018)1707427, doi:http://dx.doi.org/10.1002/adfm.201707427.
[128] R. Wei, H.Y. Chi, X. Li, D. Lu, Y. Wan, C.W. Yang, Z. Lai, Adv. Funct. Mater. 30 (2020)1907089, doi:http://dx.doi.org/10.1002/adfm.201907089.
[129] Z. Qiao, Y. Liang, Z. Zhang, D. Mei, Z. Wang, M.D. Guiver, C. Zhong, Adv. Mater. 32 (2020)2002165, doi:http://dx.doi.org/10.1002/adma.202002165.
[130] W. Li, P. Su, Z. Li, Z. Xu, F. Wang, H. Ou, J. Zhang, G. Zhang, E. Zeng, Nat. Commun. 8 (2017) 1, doi:http://dx.doi.org/10.1038/s41467-017-00544-1.
[131] E. Shamsaei, Z.-X. Low, X. Lin, A. Mayahi, H. Liu, X. Zhang, J.Z. Liu, H. Wang, ChemComm 51 (2015) 11474, doi:http://dx.doi.org/10.1039/C5CC03537F.
[132] K. Eum, C. Ma, A. Rownaghi, C.W. Jones, S. Nair, ACS Appl. Mater. Interfaces 8 (2016) 25337, doi:http://dx.doi.org/10.1021/acsami.6b08801.
[133] S. Zhou, Y. Wei, L. Li, Y. Duan, Q. Hou, L. Zhang, L.-X. Ding, J. Xue, H. Wang, J. Caro, Sci. Adv. 4 (2018)1393, doi:http://dx.doi.org/10.1126/sciadv.aau1393.
[134] N. Hara, M. Yoshimune, H. Negishi, K. Haraya, S. Hara, T. Yamaguchi, Microporous Mesoporous Mater. 206 (2015) 75, doi:http://dx.doi.org/10.1016/j.micromeso.2014.12.018.
[135] K. Eum, A. Rownaghi, D. Choi, R.R. Bhave, C.W. Jones, S. Nair, Adv. Funct. Mater. 26 (2016) 5011, doi:http://dx.doi.org/10.1002/adfm.201601550.
[136] F. Rashidi, J. Leisen, S.J. Kim, A.A. Rownaghi, C.W. Jones, S. Nair, Angew. Chem. Int. Ed. 131 (2019) 242, doi:http://dx.doi.org/10.1002/ange.201811629.
[137] E.M. Flanigen, J.M. Bennett, R.W. Grose, J.P. Cohen, R.L. Patton, R.M. Kirchner, J. V. Smith, Nature 271 (1978) 512, doi:http://dx.doi.org/10.1038/271512a0.
[138] C.-H. Cheng, T.-H. Bae, B.A. McCool, R.R. Chance, S. Nair, C.W. Jones, J. Phys. Chem. C 112 (2008) 3543, doi:http://dx.doi.org/10.1021/jp709867k.
[139] A.M. Marti, W. Wickramanayake, G. Dahe, A. Sekizkardes, T.L. Bank, D.P. Hopkinson, S.R. Venna, ACS Appl. Mater. Interfaces 9 (2017) 5678, doi:http://dx.doi.org/10.1021/acsami.6b16297.
[140] W. Li, W. Wu, Z. Li, J. Shi, Y. Xia, J. Mater. Chem. A 6 (2018) 16333, doi:http://dx.doi.org/10.1039/C8TA06083E.
[141] L. Kong, X. Zhang, Y. Liu, S. Li, H. Liu, J. Qiu, K.L. Yeung, Mater. Chem. Phys. 148 (2014) 10, doi:http://dx.doi.org/10.1016/j.matchemphys.2014.07.036.
[142] F. Cacho-Bailo, S. Catalan-Aguirre, M. Etxeberria-Benavides, O. Karvan, V. Sebastian, C. Tellez, J. Coronas, J. Membr. Sci. 476 (2015) 277, doi:http://dx.doi.org/10.1016/j.memsci.2014.11.016.
[143] W. Li, Prog. Mater. Sci. 100 (2019) 21, doi:http://dx.doi.org/10.1016/j.pmatsci.2018.09.003.
[144] J. Hou, X. Hong, S. Zhou, Y. Wei, H. Wang, AIChE J. 65 (2019) 712.
[145] I. Stassen, D. De Vos, R. Ameloot, Chem. Eur. J. 22 (2016) 14452, doi:http://dx.doi.org/10.1002/chem.201601921.
[146] P. Nian, H. Liu, X. Zhang, J. Membr. Sci. 573 (2019) 200, doi:http://dx.doi.org/10.1016/j.memsci.2018.11.076.
[147] K. Eum, M. Hayashi, M.D. De Mello, F. Xue, H.T. Kwon, M. Tsapatsis, Angew. Chem. Int. Ed. 131 (2019) 16542, doi:http://dx.doi.org/10.1002/ange.201909490.
[148] M. Hayashi, D.T. Lee, M. Dorneles de Mello, A. Boscoboinik, M. Tsapatsis, Angew. Chem. Int. Ed. (2021), doi:http://dx.doi.org/10.1002/anie.202100173.
[149] P.O. Oviroh, R. Akbarzadeh, D. Pan, R.A.M. Coetzee, T.-C. Jen, Sci. Technol. Adv. Mater. 20 (2019) 465, doi:http://dx.doi.org/10.1080/14686996.2019.1599694.
[150] R.W. Johnson, A. Hultqvist, S.F. Bent, Mater. Today 17 (2014) 236, doi:http://dx.doi.org/10.1016/j.mattod.2014.04.026.
[151] T. Tynell, M. Karppinen, Semicond. Sci. Technol. 29 (2014)043001, doi:http://dx.doi.org/10.1088/0268-1242/29/4/043001.
[152] X. Zhang, K. Wan, P. Subramanian, M. Xu, J. Luo, J. Fransaer, J. Mater. Chem. A 8 (2020) 7569, doi:http://dx.doi.org/10.1039/D0TA00406E.
[153] L. Besra, M. Liu, Prog. Mater. Sci. 52 (2007) 1, doi:http://dx.doi.org/10.1016/j.pmatsci.2006.07.001.
[154] I. Stassen, M. Styles, T. Van Assche, N. Campagnol, J. Fransaer, J. Denayer, J.-C. Tan, P. Falcaro, D. De Vos, R. Ameloot, Chem. Mater. 27 (2015) 1801, doi:http://dx.doi.org/10.1021/cm504806p.
[155] J. Liu, X.Y. Daphne Ma, Z. Wang, L. Xu, T. Xu, C. He, F. Wang, X. Lu, ACS Appl. Mater. Interfaces 12 (2020) 7442, doi:http://dx.doi.org/10.1021/acsami.9b20388.
[156] W.-J. Li, M. Tu, R. Cao, R.A. Fischer, J. Mater. Chem. A 4 (2016) 12356, doi:http://dx.doi.org/10.1039/C6TA02118B.
[157] S.D. Worrall, H. Mann, A. Rogers, M.A. Bissett, M.P. Attfield, R.A.W. Dryfe, Electrochim. Acta 197 (2016) 228, doi:http://dx.doi.org/10.1016/j.electacta.2016.02.145.
[158] R. Ameloot, L. Stappers, J. Fransaer, L. Alaerts, B.F. Sels, D.E. De Vos, Chem. Mater. 21 (2009) 2580, doi:http://dx.doi.org/10.1021/cm900069f.
[159] Z. Lai, Curr. Opin. Chem. Eng. 20 (2018) 78, doi:http://dx.doi.org/10.1016/j.coche.2018.03.002.
[160] A.M. Abdalla, S. Hossain, O.B. Nisfindy, A.T. Azad, M. Dawood, A.K. Azad, Energy Convers. Manag. 165 (2018) 602, doi:http://dx.doi.org/10.1016/j.enconman.2018.03.088.
[161] N.W. Ockwig, T.M. Nenoff, Chem. Rev. 107 (2007) 4078, doi:http://dx.doi.org/10.1021/cr0501792.
[162] Y. Alqaheem, A. Alomair, M. Vinoba, A. Perez, Int. J. Polym. Sci. 2017 (2017) 4250927, doi:http://dx.doi.org/10.1155/2017/4250927.
[163] R.W. Baker, Membrane Technology and Applications, third edition, Chichester, West Sussex, U.K, 2012.
[164] T. da Silva Veras, T.S. Mozer, A. da Silva César, Int. J. Hydrogen Energy 42 (2017) 2018, doi:http://dx.doi.org/10.1016/j.ijhydene.2016.08.219.
[165] M.-B. Hägg, R. Quinn, MRS Bull. 31 (2006) 750, doi:http://dx.doi.org/10.1557/mrs2006.188.
[166] Z. Zhou, C. Wu, B. Zhang, Ind. Eng. Chem. Res. 59 (2020) 3182, doi:http://dx.doi.org/10.1021/acs.iecr.9b06031.
[167] L. Ma, F. Svec, T. Tan, Y. Lv, J. Membr. Sci. 576 (2019) 1, doi:http://dx.doi.org/10.1016/j.memsci.2019.01.011.
[168] P. Zhao, G.I. Lampronti, G.O. Lloyd, M.T. Wharmby, S.b. Facq, A.K. Cheetham, S. A.T. Redfern, Chem. Mater. 26 (2014) 1767, doi:http://dx.doi.org/10.1021/cm500407f.

[169] J. Kim, D. Lee, J. Mater. Chem. A 4 (2016) 5205, doi:http://dx.doi.org/10.1039/C5TA10190E.
[170] A. Ersöz, Int. J. Hydrogen Energy 33 (2008) 7084, doi:http://dx.doi.org/10.1016/j.ijhydene.2008.07.062.
[171] X. Ma, Z. Wan, Y. Li, X. He, J. Caro, A. Huang, Angew. Chem. Int. Ed. 59 (2020) 20858, doi:http://dx.doi.org/10.1002/anie.202008260.
[172] X. Ma, Y. Li, A. Huang, J. Membr. Sci. 597 (2020)117629, doi:http://dx.doi.org/10.1016/j.memsci.2019.117629.
[173] P. Nian, Y. Li, X. Zhang, Y. Cao, H. Liu, X. Zhang, ACS Appl. Mater. Interfaces 10 (2018) 4151, doi:http://dx.doi.org/10.1021/acsami.7b17568.
[174] P. Raveendran, Y. Ikushima, S.L. Wallen, Acc. Chem. Res. 38 (2005) 478, doi:http://dx.doi.org/10.1021/ar040082m.
[175] J. Hou, P.D. Sutrisna, T. Wang, S. Gao, Q. Li, C. Zhou, S. Sun, H.-C. Yang, F. Wei, M. T. Ruggiero, ACS Appl. Mater. Interfaces 11 (2019) 5570, doi:http://dx.doi.org/10.1021/acsami.8b20570.
[176] X. Wang, M. Sun, B. Meng, X. Tan, J. Liu, S. Wang, S. Liu, ChemComm 52 (2016) 13448, doi:http://dx.doi.org/10.1039/C6CC06589A.
[177] P. Su, W. Li, C. Zhang, Q. Meng, C. Shen, G. Zhang, J. Mater. Chem. A 3 (2015) 20345, doi:http://dx.doi.org/10.1039/C5TA04400F.
[178] Y. Liu, J.H. Pan, N. Wang, F. Steinbach, X. Liu, J. Caro, Angew. Chem. 127 (2015) 3071, doi:http://dx.doi.org/10.1002/ange.201411550.
[179] Y. Li, C. Ma, P. Nian, H. Liu, X. Zhang, J. Membr. Sci. 581 (2019) 344, doi:http://dx.doi.org/10.1016/j.memsci.2019.03.069.
[180] P. Nian, Y. Cao, Y. Li, X. Zhang, Y. Wang, H. Liu, X. Zhang, CrystEngComm 20 (2018) 2440, doi:http://dx.doi.org/10.1039/C8CE00238J.
[181] S.R. Venna, M.A. Carreon, Chem. Eng. Sci. 124 (2015) 3, doi:http://dx.doi.org/10.1016/j.ces.2014.10.007.
[182] J.D. Figueroa, T. Fout, S. Plasynski, H. McIlvried, R.D. Srivastava, Int. J. Greenhouse Gas Control 2 (2008) 9, doi:http://dx.doi.org/10.1016/S1750-5836(07)00094-1.
[183] M. Wang, A. Lawal, P. Stephenson, J. Sidders, C. Ramshaw, Chem. Eng. Res. Des. 89 (2011) 1609, doi:http://dx.doi.org/10.1016/j.cherd.2010.11.005.
[184] D.Y.C. Leung, G. Caramanna, M.M. Maroto-Valer, Renew. Sustain. Energy Rev. 39 (2014) 426, doi:http://dx.doi.org/10.1016/j.rser.2014.07.093.
[185] S. Zhao, P.H.M. Feron, L. Deng, E. Favre, E. Chabanon, S. Yan, J. Hou, V. Chen, H. Qi, J. Membr. Sci. 511 (2016) 180, doi:http://dx.doi.org/10.1016/j.memsci.2016.03.051.
[186] R. Khalilpour, K. Mumford, H. Zhai, A. Abbas, G. Stevens, E.S. Rubin, J. Clean. Prod. 103 (2015) 286, doi:http://dx.doi.org/10.1016/j.jclepro.2014.10.050.
[187] K. Ramasubramanian, W.S.W. Ho, Curr. Opin. Chem. Eng. 1 (2011) 47, doi:http://dx.doi.org/10.1016/j.coche.2011.08.002.
[188] M. Kárászová, B. Zach, Z. Petrusová, V. Červenka, M. Bobák, M. Šyc, P. Izák, Sep. Purif. Technol. 238 (2020)116448, doi:http://dx.doi.org/10.1016/j.seppur.2019.116448.
[189] N. Prasetya, N.F. Himma, P.D. Sutrisna, I.G. Wenten, B.P. Ladewig, Chem. Eng. J. 391 (2020)123575, doi:http://dx.doi.org/10.1016/j.cej.2019.123575.
[190] X. He, M.-B. Hägg, J. Membr. Sci. 378 (2011) 1, doi:http://dx.doi.org/10.1016/j.memsci.2010.10.070.
[191] T.C. Merkel, H. Lin, X. Wei, R. Baker, J. Membr. Sci. 359 (2010) 126, doi:http://dx.doi.org/10.1016/j.memsci.2009.10.041.
[192] C. Chen, A. Ozcan, A.O. Yazaydin, B.P. Ladewig, J. Membr. Sci. 575 (2019) 209, doi:http://dx.doi.org/10.1016/j.memsci.2019.01.027.
[193] L.S. Lai, Y.F. Yeong, K.K. Lau, A.M. Shariff, RSC Adv. 5 (2015) 79098, doi:http://dx.doi.org/10.1039/C5RA12813G.
[194] D.J. Babu, G. He, J. Hao, M.T. Vahdat, P.A. Schouwink, M. Mensi, K.V. Agrawal, Adv. Mater. 31 (2019)1900855, doi:http://dx.doi.org/10.1002/adma.201900855.
[195] Y. Zhu, Q. Liu, A. Huang, Sep. Sci. Technol. 51 (2016) 883, doi:http://dx.doi.org/10.1080/01496395.2015.1135948.
[196] A.J. Brown, J.R. Johnson, M.E. Lydon, W.J. Koros, C.W. Jones, S. Nair, Angew. Chem. Int. Ed. 124 (2012) 10767, doi:http://dx.doi.org/10.1002/ange.201206640.
[197] P. Krokidas, S. Moncho, E.N. Brothers, M. Castier, H.-K. Jeong, I.G. Economou, ACS Appl. Mater. Interfaces 10 (2018) 39631, doi:http://dx.doi.org/10.1021/acsami.8b12605.
[198] R. Banerjee, A. Phan, B. Wang, C. Knobler, H. Furukawa, M. O'Keeffe, O.M. Yaghi, Science 319 (2008) 939, doi:http://dx.doi.org/10.1126/science.1152516.
[199] Y. Wang, H. Jin, Q. Ma, K. Mo, H. Mao, A. Feldhoff, X. Cao, Y. Li, F. Pan, Z. Jiang, Angew. Chem. Int. Ed. 59 (2020) 4365, doi:http://dx.doi.org/10.1002/anie.201915807.
[200] I. Amghizar, L.A. Vandewalle, K.M. Van Geem, G.B. Marin, Engineering 3 (2017) 171, doi:http://dx.doi.org/10.1016/J.ENG.2017.02.006.
[201] F.A.D. Silva, A.E. Rodrigues, AIChE J. 47 (2001) 341, doi:http://dx.doi.org/10.1002/aic.690470212.
[202] C.W. Colling, G.A. Huff Jr, J.V. Bartels, U.S. Patent, US2004/0004040, (2004).
[203] D. Liu, X. Ma, H. Xi, Y.S. Lin, J. Membr. Sci. 451 (2014) 85, doi:http://dx.doi.org/10.1016/j.memsci.2013.09.029.
[204] K. Eum, S. Yang, B. Min, C. Ma, J.H. Drese, Y. Tamhankar, S. Nair, ACS Appl. Mater. Interfaces 12 (2020) 27368, doi:http://dx.doi.org/10.1021/acsami.0c06227.
[205] J. Li, H. Lian, K. Wei, E. Song, Y. Pan, W. Xing, J. Membr. Sci. 595 (2020)117503, doi:http://dx.doi.org/10.1016/j.memsci.2019.117503.
[206] M.R. Abdul Hamid, S. Park, J.S. Kim, Y.M. Lee, H.-K. Jeong, J. Mater. Chem. A 7 (2019) 9680, doi:http://dx.doi.org/10.1039/C9TA00837C.
[207] N.T. Tran, T. Yu, J. Kim, M.R. Othman, Sep. Purif. Technol. 251 (2020)117354, doi:http://dx.doi.org/10.1016/j.seppur.2020.117354.
[208] E. Shamsaei, X. Lin, Z.-X. Low, Z. Abbasi, Y. Hu, J.Z. Liu, H. Wang, ACS Appl. Mater. Interfaces 8 (2016) 6236, doi:http://dx.doi.org/10.1021/acsami.5b12684.
[209] M.J. Lee, H.T. Kwon, H.-K. Jeong, J. Membr. Sci. 529 (2017) 105, doi:http://dx.doi.org/10.1016/j.memsci.2016.12.068.
[210] Y. Pan, W. Liu, Y. Zhao, C. Wang, Z. Lai, J. Membr. Sci. 493 (2015) 88, doi:http://dx.doi.org/10.1016/j.memsci.2015.06.019.
[211] J.H. Lee, D. Kim, H. Shin, S.J. Yoo, H.T. Kwon, J. Kim, J. Ind. Eng. Chem. 72 (2019) 374, doi:http://dx.doi.org/10.1016/j.jiec.2018.12.039.
[212] L. Sheng, C. Wang, F. Yang, L. Xiang, X. Huang, J. Yu, L. Zhang, Y. Pan, Y. Li, ChemComm 53 (2017) 7760, doi:http://dx.doi.org/10.1039/C7CC03887A.
[213] K. Huang, B. Wang, Y. Chi, K. Li, Adv. Mater. Interfaces 5 (2018)1800287, doi:http://dx.doi.org/10.1002/admi.201800287.
[214] N.T. Tran, J. Kim, M.R. Othman, Microporous Mesoporous Mater. 285 (2019) 178, doi:http://dx.doi.org/10.1016/j.micromeso.2019.05.010.
[215] N. Hara, M. Yoshimune, H. Negishi, K. Haraya, S. Hara, T. Yamaguchi, J. Membr. Sci. 450 (2014) 215, doi:http://dx.doi.org/10.1016/j.memsci.2013.09.012.
[216] J. Sun, C. Yu, H.-K. Jeong, Crystals 8 (2018) 373, doi:http://dx.doi.org/10.3390/cryst8100373.
[217] G. Ramu, M. Lee, H.-K. Jeong, Microporous Mesoporous Mater. 259 (2018) 155, doi:http://dx.doi.org/10.1016/j.micromeso.2017.10.010.
[218] S. Tanaka, K. Okubo, K. Kida, M. Sugita, T. Takewaki, J. Membr. Sci. 544 (2017) 306, doi:http://dx.doi.org/10.1016/j.memsci.2017.09.037.
[219] N. Hara, M. Yoshimune, H. Negishi, K. Haraya, S. Hara, T. Yamaguchi, J. Chem. Eng. Jpn. 49 (2018) 97, doi:http://dx.doi.org/10.1252/jcej.15we038.
[220] N.T. Tran, J. Kim, M.R. Othman, Sep. Purif. Technol. 233 (2020)116026, doi:http://dx.doi.org/10.1016/j.seppur.2019.116026.
[221] E. Song, K. Wei, H. Lian, J. Hua, H. Tao, T. Wu, Y. Pan, W. Xing, J. Membr. Sci. 617 (2021)118655, doi:http://dx.doi.org/10.1016/j.memsci.2020.118655.
[222] Q. Ma, K. Mo, S. Gao, Y. Xie, J. Wang, H. Jin, A. Feldhoff, S. Xu, J.Y.S. Lin, Y. Li, Angew. Chem. Int. Ed. 59 (2020)21909, doi:http://dx.doi.org/10.1002/anie.202008943.
[223] S. Dangwal, A. Ronte, H. Lin, R. Liu, J. Zhu, J.S. Lee, H. Gappa-Fahlenkamp, S.-J. Kim, J. Membr. Sci. 626 (2021)119165, doi:http://dx.doi.org/10.1016/j.memsci.2021.119165.
[224] Y. Zhao, Y. Wei, L. Lyu, Q. Hou, J. Caro, H. Wang, J. Am. Chem. Soc. 142 (2020) 20915, doi:http://dx.doi.org/10.1021/jacs.0c07481.
[225] R.L. Burns, W.J. Koros, J. Membr. Sci. 211 (2003) 299, doi:http://dx.doi.org/10.1016/S0376-7388(02)00430-1.
[226] H.R. Amedi, M. Aghajani, Ind. Eng. Chem. Res. 57 (2018) 4366, doi:http://dx.doi.org/10.1021/acs.iecr.7b04169.
[227] M.T. Castoldi, J.C. Pinto, P.A. Melo, Ind. Eng. Chem. Res. 46 (2007) 1259, doi:http://dx.doi.org/10.1021/ie060333q.
[228] H. Bux, C. Chmelik, R. Krishna, J. Caro, J. Membr. Sci. 369 (2011) 284, doi:http://dx.doi.org/10.1016/j.memsci.2010.12.001.
[229] O. Shekhah, R. Swaidan, Y. Belmabkhout, M. Du Plessis, T. Jacobs, L.J. Barbour, I. Pinnau, M. Eddaoudi, ChemComm 50 (2014) 2089, doi:http://dx.doi.org/10.1039/C3CC47495J.
[230] J.B. James, J. Wang, L. Meng, Y.S. Lin, Ind. Eng. Chem. Res. 56 (2017) 7567, doi:http://dx.doi.org/10.1021/acs.iecr.7b01536.
[231] P. Krokidas, M. Castier, I.G. Economou, J. Phys. Chem. C 121 (2017) 17999, doi:http://dx.doi.org/10.1021/acs.jpcc.7b05700.
[232] M. Hartmann, U. Bǿhme, M. Hovestadt, C. Paula, Langmuir 31 (2015) 12382, doi:http://dx.doi.org/10.1021/acs.langmuir.5b02907.
[233] D.-L. Chen, N. Wang, C. Xu, G. Tu, W. Zhu, R. Krishna, Microporous Mesoporous Mater. 208 (2015) 55, doi:http://dx.doi.org/10.1016/j.micromeso.2015.01.019.
[234] R. Lyndon, W. You, Y. Ma, J. Bacsa, Y. Gong, E.E. Stangland, K.S. Walton, D.S. Sholl, R.P. Lively, Chem. Mater. 32 (2020) 3715, doi:http://dx.doi.org/10.1021/acs.chemmater.9b04177.
[235] M. Gehre, Z. Guo, G. Rothenberg, S. Tanase, ChemSusChem 10 (2017) 3947, doi:http://dx.doi.org/10.1002/cssc.201700657.
[236] F. Hillman, M.R. Abdul Hamid, P. Krokidas, S. Moncho, E.N. Brothers, I.G. Economou, H.-K. Jeong, Angew. Chem. Int. Ed. (2021), doi:http://dx.doi.org/10.1002/anie.202015635.
[237] W. Wu, J. Su, M. Jia, Z. Li, G. Liu, W. Li, Sci. Adv. 6 (2020)eaax7270, doi:http://dx.doi.org/10.1126/sciadv.aax7270.
[238] O. Karagiaridi, M.B. Lalonde, W. Bury, A.A. Sarjeant, O.K. Farha, J.T. Hupp, J. Am. Chem. Soc. 134 (2012) 18790, doi:http://dx.doi.org/10.1021/ja308786r.
[239] L. Lang, F. Banihashemi, J.B. James, J. Miao, J.Y.S. Lin, J. Membr. Sci. 619 (2021) 118743, doi:http://dx.doi.org/10.1016/j.memsci.2020.118743.
[240] M. Lalonde, W. Bury, O. Karagiaridi, Z. Brown, J.T. Hupp, O.K. Farha, J. Mater. Chem. A 1 (2013) 5453, doi:http://dx.doi.org/10.1039/C3TA10784A.
[241] Z. Yin, S. Wan, J. Yang, M. Kurmoo, M.-H. Zeng, Coord. Chem. Rev. 378 (2019) 500, doi:http://dx.doi.org/10.1016/j.ccr.2017.11.015.
[242] J. Sun, L. Semenchenko, W.T. Lim, M.F.B. Rivas, V. Varela-Guerrero, H.-K. Jeong, Microporous Mesoporous Mater. 264 (2018) 35, doi:http://dx.doi.org/10.1016/j.micromeso.2017.12.032.
[243] J. Schoenmakers, Post-Synthetic Modification of Zeolitic Imidazolate Framework-8 (ZIF-8) via Cation Exchange, Master Thesis, Universiteit Utrecht, 2016.
[244] X.C. Huang, Y.Y. Lin, J.P. Zhang, X.M. Chen, Angew. Chem. Int. Ed. 45 (2006) 1557, doi:http://dx.doi.org/10.1002/anie.200503778.

[245] Y.Q. Tian, Y.M. Zhao, Z.X. Chen, G.N. Zhang, L.H. Weng, D.Y. Zhao, Chem. Eur. J. 13 (2007) 4146, doi:http://dx.doi.org/10.1002/chem.200700181.
[246] D.W. Lewis, A.R. Ruiz-Salvador, A. Gómez, L.M. Rodriguez-Albelo, F.-X. Coudert, B. Slater, A.K. Cheetham, C. Mellot-Draznieks, CrystEngComm 11 (2009) 2272, doi:http://dx.doi.org/10.1039/B912997A.
[247] J. Jiang, Curr. Opin. Green Sustain. Chem. 16 (2019) 57, doi:http://dx.doi.org/10.1016/j.cogsc.2019.02.002.
[248] C. Zhang, K. Zhang, L. Xu, Y. Labreche, B. Kraftschik, W.J. Koros, AIChE J. 60 (2014) 2625, doi:http://dx.doi.org/10.1002/aic.14496.
[249] G. Liu, V. Chernikova, Y. Liu, K. Zhang, Y. Belmabkhout, O. Shekhah, C. Zhang, S. Yi, M. Eddaoudi, W.J. Koros, Nat. Mater. 17 (2018) 283, doi:http://dx.doi.org/10.1038/s41563-017-0013-1.
[250] A. Knebel, A. Bavykina, S.J. Datta, L. Sundermann, L. Garzon-Tovar, Y. Lebedev, S. Durini, R. Ahmad, S.M. Kozlov, G. Shterk, M. Karunakaran, I.D. Carja, D. Simic, I. Weilert, M. Klüppel, U. Giese, L. Cavallo, M. Rueping, M. Eddaoudi, J. Caro, J. Gascon, Nat. Mater. 19 (2020) 1346, doi:http://dx.doi.org/10.1038/s41563-020-0764-y.
[251] S. Park, H.-K. Jeong, J. Membr. Sci. 612 (2020)118429, doi:http://dx.doi.org/10.1016/j.memsci.2020.118429.
[252] M.W. Niu, G.P. Rangaiah, Chem. Eng. Process 108 (2016) 164, doi:http://dx.doi.org/10.1016/j.cep.2016.07.013.
[253] D. Fairen-Jimenez, S.A. Moggach, M.T. Wharmby, P.A. Wright, S. Parsons, T. Duren, J. Am. Chem. Soc. 133 (2011) 8900, doi:http://dx.doi.org/10.1021/ja202154j.
[254] Y. Peng, W. Yang, Adv. Mater. Interfaces 7 (2020)1901514, doi:http://dx.doi.org/10.1002/admi.201901514.